PennState
Applied Research Laboratory

TECHNICAL REPORT

Laser Induced Fluorescence (LIF) Nondestructive Evaluation of Incipient Heat Damage in Polymer Matrix Composites, A2476

By

D. W. Merdes, C. M. Bowie, C. A. Moose

REPORT DOCUMENTATION PAGE

Form Approved
OMB No. 0704-0188

PLEASE DO NOT RETURN YOUR FORM TO THE ABOVE ORGANIZATION.

1. REPORT DATE *(DD-MM-YYYY)*	2. REPORT TYPE	3. DATES COVERED *(From - To)*
15-02-2017	Final	Oct 2011 - Jul 2016

4. TITLE AND SUBTITLE
Laser Induced Fluorescence (LIF) Nondestructive Evaluation of Incipient Heat Damage in Polymer Matrix Composites

5a. CONTRACT NUMBER
All listed in Block 13

5b. GRANT NUMBER
N/A

5c. PROGRAM ELEMENT NUMBER

6. AUTHOR(S)
Merdes, Daniel W.
Bowie, Christopher M.
Moose, Clark A.

5d. PROJECT NUMBER
A2476

5e. TASK NUMBER
N/A

5f. WORK UNIT NUMBER
N/A

7. PERFORMING ORGANIZATION NAME(S) AND ADDRESS(ES)
The Pennsylvania State Univesity
The Applied research Laboratory
PO Box 30
State College PA 16804-0030

8. PERFORMING ORGANIZATION REPORT NUMBER
TR 16-003

9. SPONSORING/MONITORING AGENCY NAME(S) AND ADDRESS(ES)
Office of Naval Research (ATTN: Mr. John Carney)
Industrial & Corporate Programs
875 North Randolph Street, Suite 1425
Arlington VA 22203-1995

10. SPONSOR/MONITOR'S ACRONYM(S)

11. SPONSOR/MONITOR'S REPORT NUMBER(S)

12. DISTRIBUTION/AVAILABILITY STATEMENT
UNLIMITED/UNLIMITED

13. SUPPLEMENTARY NOTES
Data Supplement CD contents are posted at archival web site https://doi.org/10.18113/S15K5T. Supersedes ARL TM 15-010 with associated CD.
Applicable contract numbers: N00024-02-D-6604, DO 749; N00024-12-D-6402, DO 18; N00024-12-D-6604, DO 30 & 144.

14. ABSTRACT
Fluorescence spectra were measured against four sets of polymer matrix composite (PMC) specimens that had been heated under controlled conditions of time and temperature at the Naval Air Systems Command (NAVAIR). Each set consisted of specimens of a different fiber-reinforced PMC material: AS4/3501 6 5HS; AS4/3501 6 Uni-Tape; IM7/5250 4 Uni-Tape; and IM7/977 3 Uni-Tape. A chemometric model was developed to correlate changes in spectral features with changes in strength, which NAVAIR had measured according to the short-beam shear (SBS) standard after performing the heat treatments. That model is shown to be able to predict whether a given specimen had been degraded to below 80% of original strength based on its fluorescence spectrum. All steps of the chemometric model are fully described, and the complete data are provided on the CD that accompanies the report.

15. SUBJECT TERMS
Polymer Matrix Composites, Incipient Heat Damage, Laser Induced Fluorescence, Short Beam Shear, Chemometric Analysis

16. SECURITY CLASSIFICATION OF:			17. LIMITATION OF ABSTRACT	18. NUMBER OF PAGES	19a. NAME OF RESPONSIBLE PERSON
a. REPORT	b. ABSTRACT	c. THIS PAGE			Daniel W. Merdes
U	U	U	UU	59	19b. TELEPHONE NUMBER *(Include area code)* (814) 863-4145 Email dwm@arl.psu.edu

Reset

The Pennsylvania State University
The Applied Research Laboratory
PO Box 30
State College PA 16804-0030

Laser Induced Fluorescence (LIF) Nondestructive Evaluation of Incipient Heat Damage in Polymer Matrix Composites, A2476

by

Daniel W. Merdes, Christopher M. Bowie*, and Clark A. Moose

*Current Affiliation: Ocean Optics, Inc., 4301 Metric Drive, Winter Park FL 32792

Technical Report TR 16-003

February 15, 2017

Supported by: Office of Naval Research
Contract Numbers:
N00024-02-D-6604, DO 749
N00024-12-D-6402, DO 18
N00024-12-D-6604, DO 30 & 144

Paul E. Sullivan, Director
Applied Research Laboratory

Intentionally Blank

Abstract

Fluorescence spectra were measured against four sets of polymer matrix composite (PMC) specimens that had been heated under controlled conditions of time and temperature at the Naval Air Systems Command (NAVAIR). Each set consisted of specimens of a different carbon-fiber-reinforced PMC material: AS4/3501-6 5HS; AS4/3501-6 Uni-Tape; IM7/5250-4 Uni-Tape; and IM7/977-3 Uni-Tape. A chemometric model was developed to correlate changes in spectral features with changes in strength, which NAVAIR had measured according to the short-beam shear (SBS) standard after performing the heat treatments. That model is shown to be able to predict whether a given specimen had been degraded to below 80% of original strength based on its fluorescence spectrum. All steps of the chemometric model are fully described, and the complete data are provided on the CD that accompanies the report.

Intentionally Blank

Executive Summary

Polymer matrix composites (PMCs) have come into widespread use to construct the wing, fuselage, and other major structural components of high-performance military aircraft, replacing metals such as aluminum, magnesium, and titanium that became prevalent in the twentieth century. This design trend stems mainly from the high strength-to-weight ratio and improved resistance to fatigue and corrosion of those materials relative to metals. But PMCs are prone to substantial loss of strength and flexibility from exposures to high heat fluxes from such contingencies as fire, engine exhaust gases from nearby aircraft, equipment overheats and even routine operations. These materials can suffer substantial degradation in strength and other properties without exhibiting any evidence of discoloration, delaminations or other indications either visually or through traditional NDE methods—a condition that has come to be termed *incipient heat damage*. There is currently no fielded NDE method to assess incipient heat damage, resulting in expensive aircraft composite components being scrapped as a precaution. If the heat damage could be assessed and found to be limited to a small volume of the composite component in question, it can be repaired in many cases. Besides the substantial cost saving, repairing an existing component also greatly reduces the down time of the aircraft, allowing the depot to return it to service within weeks instead of months. There is often a long lead-time to procure a replacement component, and once delivered, its installation will likely require considerable effort and expenditure.

This report describes a laboratory apparatus developed for measurement of fluorescence data against specimens of composite material that have suffered incipient heat damage under controlled thermal conditions. Using that apparatus, spectra were measured against four different sets of NAVAIR Composite Heat Damage Standards, representing four composite materials used on structural components of US Naval aircraft:

- AS4/3501-6 (Five-harness satin (5HS) Fabric-reinforced, Epoxy matrix)
- IM7/5250-4 (Uni-Tape-reinforced, Bismaelimide (BMI) matrix)
- AS4/3501-6 (Uni-Tape-reinforced, Epoxy matrix)
- IM7/977-3 (Uni-Tape-reinforced, Toughened Epoxy matrix)

A chemometric analysis methodology was developed to correlate changes in spectral signatures with degradation in strength measured according to the short-beam-shear standard. The steps of that analysis methodology are described, and it is shown to be able to correctly assess, based on a fluorescence spectrum, whether a given specimen has suffered a degradation in strength to below 80% of its original value.

Finally, technology goals for a follow-on project to design and fabricate a field-portable prototype non-destructive evaluation system are defined by the project team. They include: the need for a thorough data-collection campaign; packaging into a shock-mounted, human-portable unit; optics permitting interrogation using a hand-held probe connected to the portable unit; built-in calibration to automatically adjust for spectrometer drift; and a capability to assess whether a measured spectrum has characteristics indicative of surface contamination that might cause a false reading.

Intentionally Blank

Table of Contents

Abstract iii
Executive Summary v
Table of Contents vii
List of Figures ix
List of Tables ix
List of Abbreviations xi
Acknowledgements xiii
1 Introduction 1
2 Background 3
2.1 Literature Review 3
2.2 Chemometric Analysis 4
3 Project Synopsis 7
4 Experimental 9
4.1 Apparatus 10
4.2 Material Samples 11
4.3 Data Collection 12
5 Analysis 15
5.1 Qualitative Analysis of the 5HSAS4 Spectra 15
5.2 Quantitative Analysis of the 5HSAS4 Spectra 17
5.2.1 Preprocessing 17
5.2.1.1 Normalization 17
5.2.1.2 Trimming 18
5.2.1.3 Culling 18
5.2.1.4 Centering 19
5.2.2 Model Generation. 20
5.2.2.1 Principal Components Analysis 20
5.2.2.2 Principal Components Regression 21
5.2.3 Validation. 23
5.3 Analysis of the BMI Spectra 25
5.4 Analysis of the AS4 and 977 Spectra 28
6 Conclusion 31
7 References 33
APPENDIX A. Accessing Data on the NAVAIR Composite Heat Damage Standards A-1
APPENDIX B. Example Spectral Data File B-1
APPENDIX C. Accessing the Spectral Data Measured in this Study C-1

APPENDIX D. The Data Supplement D-1
APPENDIX E. Irradiation Through Optical Fiber E-1

List of Figures

Figure 1. The LIF NDE Gen I Instrument. 4
Figure 2. Data from Commercial-Grade Spectrometers. 9
Figure 3. The LIF NDE Gen II Breadboard with Components Labeled. 10
Figure 4. NAVAIR Heat Damage Specimens. 11
Figure 5. A Typical Fluorescence Spectrum. 13
Figure 6. The Effect of Normalization. 15
Figure 7. Treatment Temperature Effect on 5HSAS4 Spectra. 16
Figure 8. Distortion from Surface Contamination. 18
Figure 9. The Response Matrix for 5HSAS4. 19
Figure 10. Significance of the Nine Principal Components. 21
Figure 11. The Model Fit to 5HSAS4 Spectra. 22
Figure 12. Validation Chart for 5HSAS4 Spectra Measured 2 June 2014. 24
Figure 13. Validation Chart for 5HSAS4 Spectra Measured 6 June 2014. 24
Figure 14. Treatment Temperature Effect on BMI Spectra. 25
Figure 15. Response Matrix for BMI Spectra Measured 4 June 2014. 26
Figure 16. Validation Chart for BMI Spectra Measured 4 June 2014. 27
Figure 17. Validation Chart for BMI Spectra Measured 29-30 May 2014. 27
Figure 18. Response Matrix for AS4. 29
Figure 19. Validation Chart for AS4. 29
Figure 20. Response Matrix for 977. 30
Figure 21. Validation Chart for 977. 30
Figure E1. Apparatus Modification for Irradiation Through Optical Fiber. E-2
Figure E2. Fiber Cable Intercepting Laser Beam. E-2
Figure E3. Specimen Irradiated by Probe. E-2
Figure E4. Direct- and Fiber-Irradiated Spectra Compared. E-3

List of Tables

Table 1. PMCs Used in This Study 12
Table 2. Data Collection Runs 14

Intentionally Blank

List of Abbreviations

ARL Penn State	The Applied Research Laboratory at The Pennsylvania State University
BMI	Bismaleimide
CCD	Charge Coupled Device
COTS	Commercial Off-The-Shelf
DoD	Department of Defense
DRIFT	Diffuse Reflectance Infrared Fourier Transform
FRC-East	Fleet Readiness Center-East (at MCAS Cherry point NC)
iMAST	Institute for Manufacturing and Sustainment Technologies (ONR MANTECH at ARL Penn State)
LIF	Laser-Induced Fluorescence
MANTECH	MANufacturing TECHnology
MCAS	Marine Corps Air Station
NAVAIR	Naval Air Systems Command
NDE	Non-Destructive Evaluation
ONR	Office of Naval Research
ORNL	Oak Ridge National Laboratory
PMC	Polymer Matrix Composite
PMT	PhotoMultiplier Tube
R&D	Research and Development
SBS	Short-Beam Shear

Intentionally Blank

Acknowledgements

This work was funded by Office of Naval Research through its center of excellence, the Institute for Manufacturing and Sustainment Technologies (iMAST), under the following contract numbers with the Naval Sea Systems Command:

N00024-02-D-6604, Delivery Order 749
N00024-12-D-6402, Delivery Order 18
N00024-12-D-6604, Delivery Orders 30 & 144

The opinions, findings, conclusions, and recommendations expressed in this material are those of the authors and do not necessarily reflect the views of the Naval Sea Systems Command, the Office of Naval Research, or our collaborators at the Naval Air Systems Command (NAVAIR).

We wish to acknowledge the invaluable assistance of Dr. Raymond Meilunas and his staff at NAVAIR 4.3.4.4 for technical assistance and access to the NAVAIR Composite Heat Damage Standards described in this report, along with details he provided on how those standards are prepared, maintained, and made available to research groups such as ours. Mr. Robert Kestler (NAVAIR 4.0) and his staff at FRC-East, MCAS Cherry Point NC provided valuable guidance on the relevant operational requirements. We also acknowledge Dr. Michael Zugger of ARL Penn State for his assistance with apparatus instrumentation and participation in the data collection runs between 29 May and 6 June 2015. Daniel Sills of ARL Penn State assisted with data collection from 28 to 30 July 2015. Derek Lang of ARL Penn State performed statistical analyses of some of our preliminary data.

Intentionally Blank

1 Introduction

Polymer matrix composites (PMCs) have come into widespread use to construct the wing, fuselage, and other major structural components of high-performance military aircraft, replacing metals such as aluminum, magnesium, and titanium that were prevalent in the twentieth century. This design trend stems mainly from the high strength-to-weight ratio and improved resistance to fatigue and corrosion of those materials relative to metals. Unfortunately, PMCs are prone to substantial loss of strength and flexibility from exposure, or repeated exposures, to high heat fluxes from such contingencies as fire, engine exhaust gases from nearby aircraft, equipment overheats, and even routine operations. Up to a point, these materials can experience substantial degradation in strength and other properties without exhibiting any evidence of discoloration, delaminations or other indications—a condition that has come to be termed *incipient heat damage* (Matzkanin & Hansen, 1998). Instances of mechanical strength degradation from incipient heat damage in aircraft PMCs exceeding 60% have been reported (Fisher *et al.*, 1995). Currently, there is no fielded non-invasive means to assess incipient heat damage. This inability to properly identify the extent of incipient heat damage can result in expensive aircraft composite components being scrapped as a precaution. If the heat damage could be assessed and found to be limited to a small volume of the composite component in question, it could be repaired in many cases. Besides the substantial cost saving, repairing an existing component also greatly reduces the down time of the aircraft, allowing the depot or unit to return it to service within weeks instead of months. There is often a long lead-time to procure a replacement component, and once delivered, its installation will likely require considerable effort and expenditure.

This report documents our research to develop a non-destructive evaluation (NDE) capability to use *Laser-Induced Fluorescence* (LIF) to assess incipient heat damage in four different PMC materials. Our results demonstrate the feasibility of employing LIF using commercial off-the-shelf (COTS) components in a laboratory environment. Further data collection, analysis, and engineering is proposed to develop a field-portable prototype suitable for employment at aircraft depots, aboard aircraft carriers, and at other operational venues.

Intentionally Blank

2 Background

Below, we provide a brief survey of the literature relating to non-destructive evaluation of incipient heat damage in polymer matrix composites and an overview of the use of chemometric analysis to develop an NDE assessment capability.

2.1 Literature Review

Kerr & Haskins (1984) appear to have first reported on what is now termed incipient heat damage of PMCs in the refereed science and engineering literature while their experimental study on environmental thermal aging was still underway, preceded by their government report (1980). Their research dealt with long-term degradation during normal operations. They subsequently prepared a detailed report on their findings (1987), which Haskins (1989) later summarized. Luoma & Rowland (1986) and earlier investigators have published studies on degradation of pure epoxy materials by heating and other forms of exposure. Bowie's master's thesis (2017) includes a review of the scientific and engineering literature on incipient heat damage in PMCs and the various means that have been studied to assess such damage by NDE methods.

A group of researchers at, or in collaboration with, Oak Ridge National Laboratory (ORNL) was apparently the first to perform detailed studies of heat damage to PMCs induced by short-term exposure to temperatures above what they were designed to withstand. In 1990 they first reported on experiments in which PMC specimens were heat-treated under controlled conditions and then tested for strength by various standard methods (Frame *et al.*, 1990). Those PMC specimens were then examined using a variety of NDE techniques, the results of which were correlated with the strength data. While LIF was not one of the techniques treated in their first report, later that year the group published another report evaluating two spectroscopic techniques: *Laser-Pumped Fluorescence* (another term for LIF) and *Diffuse Reflectance Infrared Fourier Transform Spectroscopy* (DRIFT) (Janke *et al.*, 1990). They subsequently published what appears to be the first detailed study on the use of LIF for this purpose in the referred literature (Fisher *et al.*, 1995), and went on to develop an experimental imaging apparatus for analysis of incipient heat damage in PMCs from a standoff distance—seemingly on the order of one to a few meters (Fisher *et al.*, 1997). In the mid-2000s Galt Technologies, Inc. (Galt) and ORNL developed, under sponsorship of the Office of Naval Research (ONR), a human-portable instrument for performing NDE for incipient heat damage on PMCs using LIF (Figure 1)—apparently the first reported use of automated chemometric analysis to assess incipient heat damage in PMCs based on their fluorescence spectra. That instrument in 2008 received recognition from a prestigious technology publication as one of the year's top 100 technology innovations (R&D 100 Awards, 2008 a,b,c).

The Galt instrument—referred to herein as the *Generation I LIF NDE Prototype* (or *Gen I Prototype* for short)—consists of a 405 nm diode laser, a grating spectrometer, a 32-element linear photomultiplier (PMT) array, analog-to-digital converter, detection electronics, and power supply. A laptop computer accesses data from the unit through a USB connection, performs the chemometric analysis using custom software, and displays results.

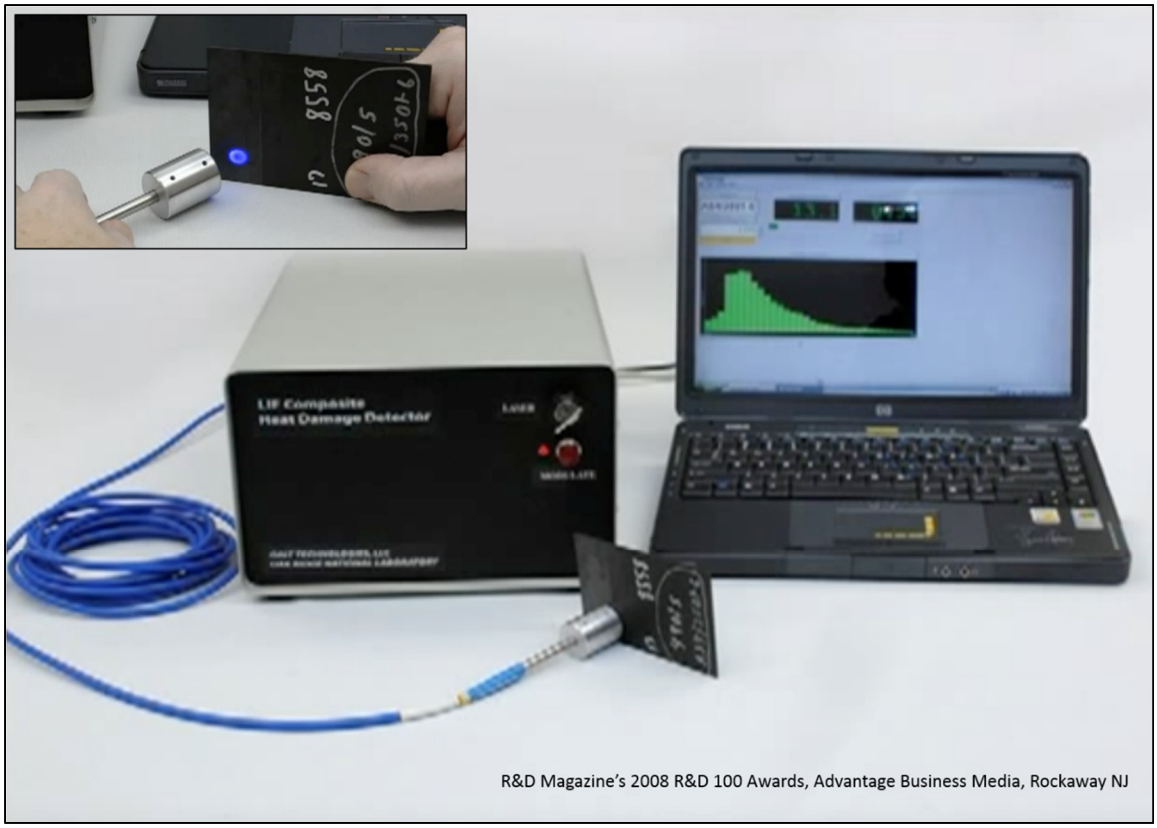

Figure 1. The LIF NDE Gen I Instrument in use to assess incipient heat damage in a test specimen. The inset shows the effect of the laser beam upon the specimen when the probe when held a short distance away. Photos clipped from YouTube video posted by R&D Magazine and used with permission (R&D 100 Awards, 2008 c).

The interrogation radiation is transmitted through a fiber-optic cable to a hand-held probe. That probe, when held flush against a surface, irradiates a spot on the surface from a single, center-mounted optical fiber. Six fibers encircling the center collect fluorescence emitted from the irradiated spot and transmit that light back into the entrance port of the unit's spectrometer. The interrogation radiation is generated by a 405 nm diode laser operating at 5 mW, the maximum power allowable under applicable personnel safety restrictions stipulating adherence to the former ANSI Class 3A standard—which remains the limit under the now-applicable Class 3R standard (*ANSI Z136.1–2007*).

2.2 Chemometric Analysis

When one attempts to correlate chemical data (such as spectra as in this study) with some property of a substance or material (such as the strength of PMCs as in this study), one is engaging in the practice called *chemometrics* (Beebe et al., 1998). Typically, though not necessarily, direct measurement of the property of interest entails inflicting damage to or even destruction of the specimen under study, while the chemical data can be measured non-destructively. Although chemometrics can be used in a strictly analytical manner to derive correlations between the property of interest and the chemical data, the usual

motivation is to devise a means to estimate the property of interest based on a non-destructive measurement that can be *readily* obtained *in the operational environment* (i.e. the environment where the object of interest would be located, such as a hangar in the case of aircraft). Four major steps can be envisioned in order to achieve that end:

1. One must obtain or devise an apparatus that can be used to support the research required to develop the required measurement methodology. In our case, this is a laboratory-based apparatus that lends itself to adjustment of the experimental conditions.
2. One must collect enough data to support development and validation of an assessment algorithm.
3. One must develop a chemometric algorithm that can be used to derive the values of the statistical parameters that characterize the manner in which the property data are correlated with the chemical data, and then validate that so-called *chemometric model* by demonstrating its efficacy in estimating the property data based on chemical data that were *not* used to derive the model parameters.
4. Finally, one must *package* the capability into an instrument that can be used in the applicable operational environment. This is primarily a matter of engineering development of the instrumentation and operating software.

As will be seen, we have achieved the first three steps toward developing a chemometric analysis capability for assessment of incipient heat damage to PMCs, and propose to pursue the follow-on development necessary to package that capability into an instrument that can be used in the operational environments applicable to Naval aviation.

Intentionally Blank

3 Project Synopsis

NAVAIR representatives provided a number of requirements for configuration and operating improvements at the beginning of this project. They emphasized the need to expand the analysis capability beyond the current limited suite of composite materials to include newer material systems now being employed in the latest naval aircraft, such as CH-53K, F-35, V-22, and F-18. Those representatives included a member of the Navy R&D community—Dr. Raymond Meilunas of NAVAIR's Polymers and Composites Branch (NAVAIR 4.3.4.4.)—as well as NAVAIR's operational support community led by Mr. Robert Kestler (NAVAIR 4.0T) and Bradley Hartman (NAVAIR 4.3.4.4) of the Fleet Readiness Center East (FRCE) at Marine Corps Air Station Cherry Point (MCAS Cherry Point).

One cannot replicate the Galt unit without access to its custom electronics boards and software. Rather than attempt to copy its design component-for-component, we opted to pursue a simpler design employing COTS components that are viable for future integration in a portable system making no special modifications. With funding from the ONR ManTech program Center of Excellence at ARL Penn State (iMAST) we developed an apparatus—which we call the *LIF NDE Generation II Breadboard Apparatus* (or *Gen II Breadboard* for short)—on an optical table in our laboratory. Using a basic chemometric algorithm, which we developed and coded ourselves, we have demonstrated that the modern COTS portable spectrometer incorporated into our apparatus can collect LIF spectral data over short time intervals with a noise level low enough to be used for accurate spectral-mechanical property assessment correlations. In this report we show that it can be used to assess whether any of four different PMC materials have experienced incipient heat damage severe enough to degrade strength below 80% of its original value. This was accomplished without resorting to a custom PMT array spectrometer design as in the Gen I system. Unlike the Galt unit, we rely on the spectrometer's built-in CCD array and processing firmware. We operate the laser in continuous mode and specify the spectrometer's integration time using the control software supplied by its manufacturer; however, our laser can be modulated, and the spectrometer synchronized to it, should it be desired to operate the apparatus in typical ambient lighting conditions.

Our iMAST-approved project plan defined this effort as leading to development of a portable next-generation prototype; however, the limited iMAST funding was only intended to support a proof-of-principle study to be taken as far as a laboratory demonstration. That task was to be followed by a project to develop a portable *LIF NDE Generation II Prototype* (*Gen II Prototype*) under other funding. Thus, this document serves as the final report for the iMAST effort as well as the basis of a proposal for the Gen II Prototype development and other follow-on efforts.

Intentionally Blank

4 Experimental

Prior to assembling the Gen II Breadboard apparatus described below in its final form, we experimented with two less-expensive commercial spectrometers; Figure 2 shows typical spectra measured by those instruments. Early results using the Ocean Optics *Jaz* spectrometer yielded spectra that, though noisy, showed visibly-discernable differences in the spectra of test specimens we prepared ourselves. We then used the older, more-sensitive Ocean Optics *HR 2000* spectrometer with an open apparatus we developed using careful optical design principles (described below). We thereby obtained improved spectra which, however, were obviously noisy and misshapen even when the integration time was increased to as long as ten seconds.

We then accepted an offer from Ocean Optics to try their scientific-grade *QE 65 Pro* portable spectrometer, which proved to yield high-quality spectra at integration times as short as one second.

The account below treats our final Gen II Breadboard design and the character of the data measured using that apparatus. Bowie's master's thesis (2017) includes a discussion of the development path leading to the Gen II Breadboard and a more detailed design description.

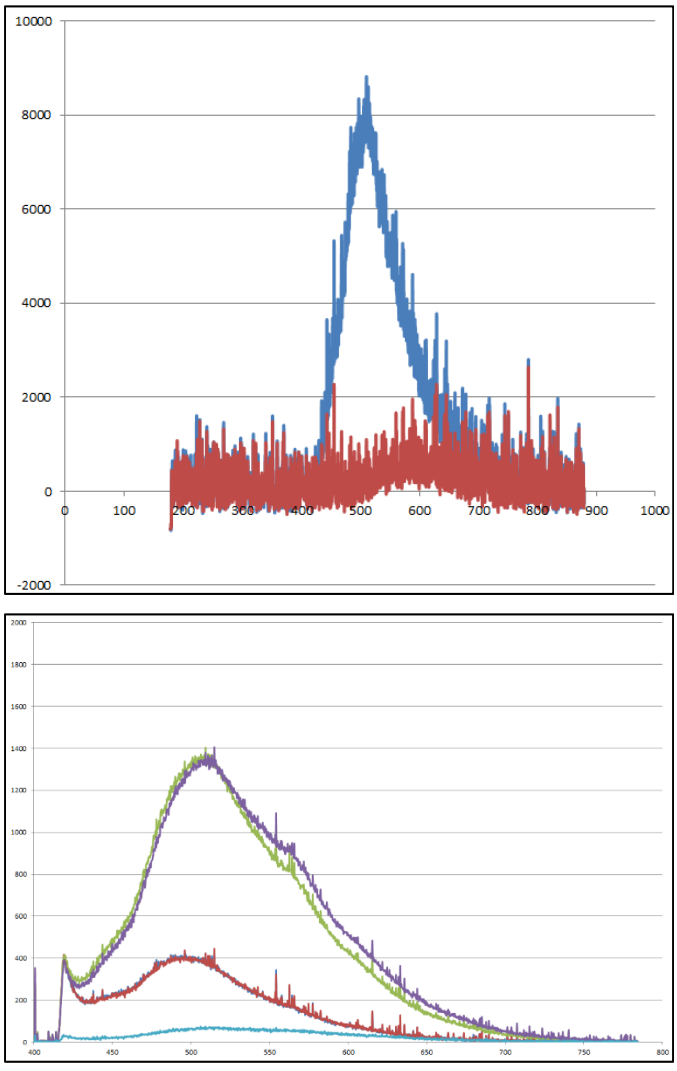

Figure 2. Data from Commercial-Grade Spectrometers. Top, using the Ocean Optics *Jaz*; bottom, using Ocean Optics *HR 2000*. While much improved, the *HR 2000* data was judged to be marginal for analysis purposes: the "spikes" and "wiggles" in the data traces arise from operating the spectrometer at light levels below its design specifications. Compare with the *QE 65 Pro* data in Figures 5, 6, 7, and 8.

4.1 Apparatus

As is typical of a fluorescence apparatus, the Gen II Breadboard consists of two major subsystems—one to irradiate the specimen under study, the other to collect fluorescence emitted from the specimen into a spectrometer. In Figure 3, an overhead view of the Gen II Breadboard, the irradiation subsystem appears in the center diagonally aligned from lower right to upper left. The laser is mounted on a post and oriented to irradiate the specimen. Three translation stages are mounted on an optical track aligned under the laser beam to support components for control and monitoring of the irradiation beam. A pickoff window is mounted on one of the stages to sample the beam for power measurement, while the other two stages are empty because this particular laser has built-in optics for beam control. Those stages would perhaps hold optics for beam expansion, aperture control, and/or focusing when used with a different laser or other light source.

The collection optics are mounted on the optical track bolted parallel to the left edge of the optical table in the figure. A special-purpose lens assembly called a *collimator* is attached to the end of the fiber optic cable from the spectrometer, and there are another two lenses we have termed the *collector* and *displacer* between the specimen and the collimator. Those three elements are mounted on separate translation stages and are positioned to focus the *collection spot* (the circular region on the specimen from which fluorescence is collected) onto the face of the optical fiber behind the collimator. One sets the diameter of the collection spot by appropriately adjusting the positions of the collector, displacer, and

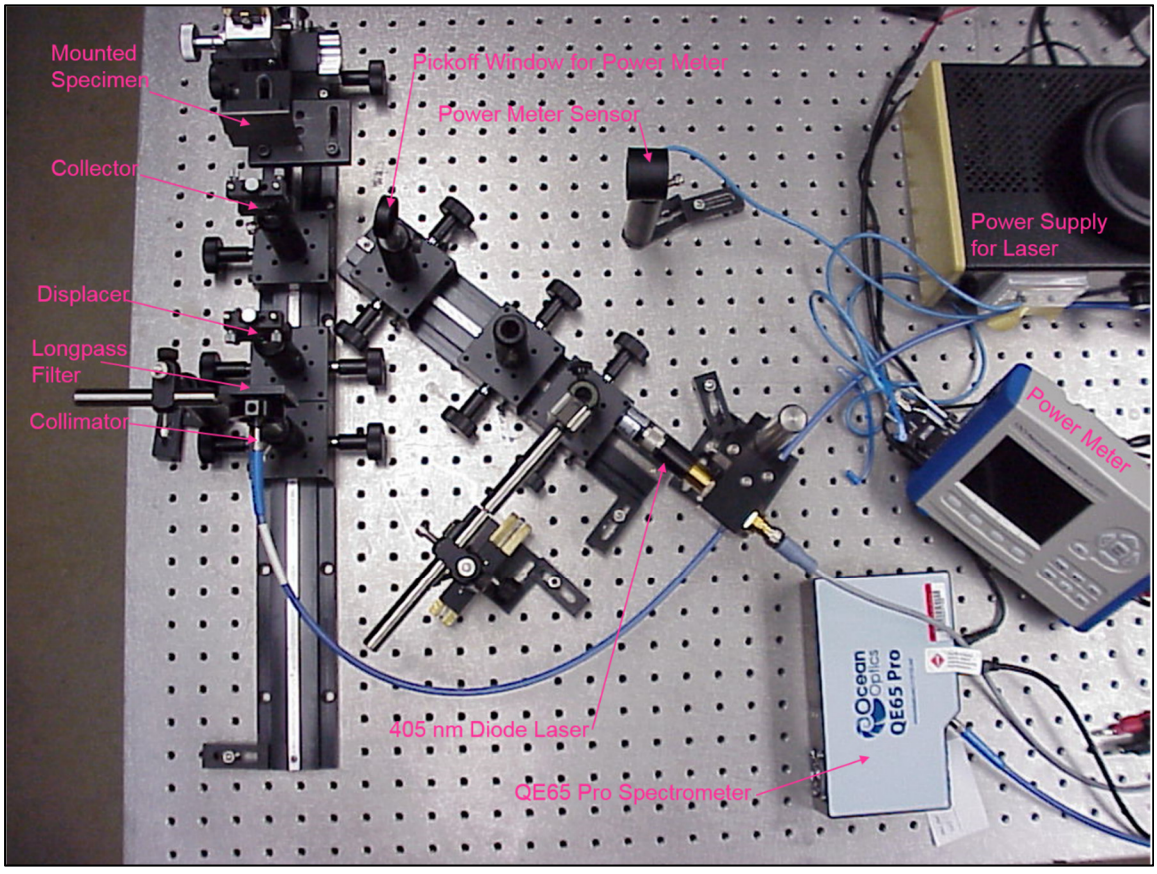

Figure 3. The LIF NDE Gen II Breadboard with Components Labeled.

collimator. The collection optics were designed to permit the collection spot diameter to be varied between 2 and 10 mm. A longpass filter is mounted in front of the collimator to reject incident light scattered from the specimen at wavelengths below 415 nm.

4.2 Material Samples

All spectra documented in this report were measured against sets of *NAVAIR Composite Heat Damage Standards* prepared by the NAVAIR Polymers and Composites Branch (NAVAIR 4.3.4.4) in previous programs. Those standards consist of sets of aerospace grade composite laminate specimens that were heat-damaged in a controlled fashion at a variety of time-temperature conditions over the incipient thermal damage temperature range. After heat treatment, the mechanical properties were measured from a section of each time-temperature control. The standards are specifically intended to provide a common basis for developing correlations between mechanical strength and spectral features measured using emerging NDE spectroscopic techniques for composite heat damage assessment. NAVAIR lends the standards to Department of Defense (DoD) programs developing new NDE methods to facilitate direct comparison of the capabilities of the competing approaches. A given standard set is characterized by the specific composite material system (which include the major types certified for use on DoD aircraft), the specifics of how the specimens were heat damaged (the temperatures to which they were thermally treated and the exposure time), and their mechanical strength values after treatment as measured by the *Short Beam Shear* (SBS) mechanical test method (ASTM D2344, 2013). (NAVAIR Heat Damage Standards)

The NAVAIR Composite Heat Damage Standards come in two different sample configurations, both shown in Figure 4. One configuration consists of a set of 16 ply, 3″×4″ laminates that were heat-damaged at different time-temperature conditions. For each laminate there is also a set of SBS shear specimens that were machined from the edge of the original heat-treated 4″×4″ laminate and mechanically tested. LIF spectra are measured repeatedly from different collection spots on the same laminate (now 3″×4″) and correlated to the SBS results. The other heat damage standard configuration consists of a set of separate heat-damaged SBS specimens. Those SBS specimens were first machined from a large, pristine laminate panel; then, subsets (typically ten specimens each) were treated at the different time-temperature conditions. After subjection to thermal exposures, those specimens were mechanically tested before being made available for analysis by LIF or other methods. The two main benefits of the latter standard configuration are: 1) for each time-temperature condition the LIF spectra are now taken directly from the SBS specimens, and 2) additional non-thermal mechanical damage due to machining of the

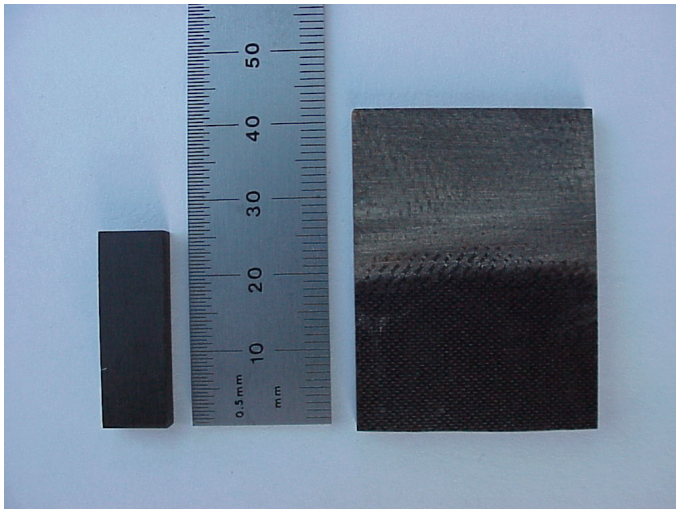

Figure 4. NAVAIR Heat Damage Specimens. Left, an SBS specimen. Right, a piece cut from a single laminate specimen.

Table 1. Polymer Matrix Composites Used in This Study

Short Descriptor	Material Description	Number of Specimens	Type	Range of Treatment Temperatures (°F)
5HSAS4	AS4/3501-6 5HS Fabric (Epoxy)	50	SBS	350 – 510
BMI	IM7/5250-4 Uni-Tape (BMI, Qualified)	70	SBS	350 – 610
AS4	AS4/3501-6 Uni-Tape (Epoxy)	9	Single	350 – 490
977	IM7/977-3 Uni-Tape (Toughened Epoxy)	4	Single	410 – 490

This table lists the four PMC materials for which spectral data was measured and analyzed in this study. The short descriptor is defined for convenience of reference within this report. Under the Type header, SBS indicates that a number of SBS specimens were provided for each different treatment, while Single indicates that only a single 3″×4″ laminate was provided for each treatment. The treatment time was 60 minutes for all specimens.

specimens is avoided. NAVAIR has demonstrated that both of these benefits contribute to more accurate spectral-mechanical correlations.

For both standard configurations, a unique identifier (label) appears on each specimen. When single 3″×4″ pieces were provided for a given standard set, there was only one specimen for each time-temperature treatment applied to the material; we took a number of spectra from that one specimen, taking care that no two collection spots overlapped. When a number of SBS specimens were provided for each treatment, we took at least one spectrum against each specimen and sometimes two or three—again taking care to avoid any overlap.

Table 1 lists the sets of NAVAIR Composite Heat Damage Standards discussed in this report. The "Material Description" column provides a complete descriptive code in the form *fiber/resin reinforcement*. Two types of carbon fiber are represented—AS4 (HexTow AS4 Product Data Sheet) and IM7 (HexTow IM7 Product Data Sheet). Three types of resin are represented—3501-6 (Hexcel 3501-6 Product Data Sheet), 5250-4 (CYCOM 5250-4 Tech Data Sheet), and 977-3 (CYCOM 977-3 Tech Data Sheet). The reinforcement refers to how the given carbon reinforcing fiber is arranged: "5HS Fabric" refers to a five-harness-satin woven mesh, while for "Uni-Tape" the reinforcing fibers are all oriented in the same direction rather than being woven.

Appendix A describes how the data NAVAIR provided on the treatments applied to the specimens in those sample sets, and their measured SBS values, are documented in the Data Supplement. For the SBS specimens, the *average* value of the SBS measurement was provided rather than the values obtained for each given specimen. For the 3″×4″ laminates, NAVAIR obtained the SBS value by cutting ten specimens from the edge, mechanically testing, and recording the average.

4.3 Data Collection

NAVAIR follows a specific protocol to prepare the surface of each specimen of a sample set prior to taking their fluorescence spectra. This protocol is critical for collecting accurate fluorescence data for two reasons: First, the preparation removes any contaminates from the surface, which is essential because the majority of potential organic contaminates are fluorescent to some degree. Second, the sanding step removes the thin (nanometer-scale)

native polymeric oxide that forms at room temperature on the composite surface over time (Haskins, 1989). This native oxide has a strong fluorescence signature, which is distinct from that obtained via thermo-oxidation of the polymer component of the composite and must be removed for accurate correlations. The protocol entails cleaning with an organic solvent (isopropyl alcohol or acetone), lightly sanding over with fine (200 grit) sandpaper, then dry wiping with a non-fabric polymer wipe such as Teflon release film or even pieces cut out from a clean, non-powdered latex or nitrile disposable glove. Cheesecloth or Kimwipes™ are never used for the dry wipe, as both leave extremely fluorescent microfibril contaminants on the composite surface. This protocol is consistent with the expected operational employment methodology: The majority of aircraft components are painted or primed; hence, they must first be sanded to expose the composite surface to be tested. In most cases, the composite medium to be tested would not have been exposed to air during thermal exposure, as a result of which the degradation mechanism will usually be strictly thermal rather than thermal-oxidative. Those two degradation cases yield different fluorescence spectra. (Meilunas, 2015)

For the two sample sets measured in late-May to early-June 2014, NAVAIR 4.3.4.4 staff performed the cleaning regimen at the Materials Laboratory at US Naval Air Station Patuxent River, then shipped them to ARL Penn State. The time between sanding and LIF analysis was only a few days, which is not an issue because it takes over a week for a substantial native oxide layer to form on the composite surface (Meilunas, 2015). For the remaining sample sets measured in July 2014, NAVAIR 4.3.4.4 personally brought the standards to our laboratory and performed the surface preparation regimen immediately before handing them over to us for spectral interrogation.

Figure 5 shows a spectrum taken against a 5HSAS4 specimen using the Gen II Breadboard. As is common for fluorescence spectra, it features a single broad peak having a positive skew; that is, the rise with increasing wavelength to the peak ordinate value is steeper than the fall back toward the abscissa. As is typical, the 405 nm irradiation wavelength establishes the lower wavelength bound of the fluorescence spectrum. The sharp *irradiation peak* that occurs slightly past 400 nm is due to incomplete filtering of the laser light scattered from the surface of the specimen; that scattering slightly distorts the spectrum up to about 700 nm. (As will be explained below, we "trim" the spectra at 450 nm to eliminate any significant influence of the irradiation peak on our quantitative analysis.)

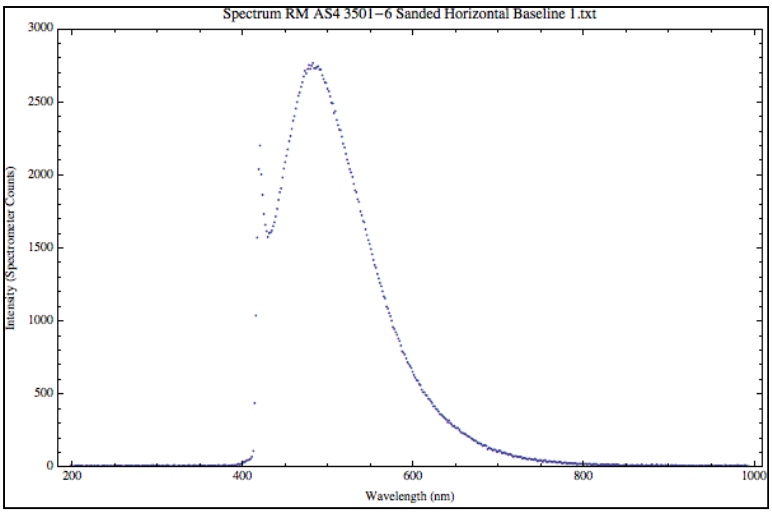

Figure 5. A Typical Fluorescence Spectrum taken against a specimen of 5HSAS4 (not heat-treated).

The values displayed in Figure 5 were input from the data file output by the operating software, *SpectraSuite*®, provided by

the spectrometer's manufacturer. Appendix B shows the structure of that plain-text file, which starts with such metadata as the date and time it was taken, the spectrometer's serial number, and various settings to be used in translating the spectrometer's raw signal output into the numerical values of a 1024-point wavelength spectrum. The value pair—wavelength (nm) and intensity (which is expressed in spectrometer "counts", a measure specific to the instrument and software)—for each point follows in sequence from low to high wavelength, with a separate record for each point. A final record placed after the last data point denotes the end of the data set.

Table 2 summarizes the data runs reported herein. Appendix C describes how, for each spectrum of each data run, certain metadata assigned by ourselves to facilitate automated analysis are documented in the Data Supplement: a unique spectrum identifier, the identifier of the specimen against which the spectrum was taken, the name assigned to the file generated for that spectrum, and a code specifying our judgment of whether that spectrum qualifies for inclusion in the analysis (more on this later). All of the *SpectraSuite*® files from each data run discussed in this report are included in the Data Supplement.

Table 2. Data Collection Runs

Data Run Identifier	Number of Spectra
5HSAS4_02Jun2014	152
5HSAS4_06Jun2014	50
BMI_29May2014	212
BMI_04Jun2014	70
AS4_30Jun2014	135
977_29Jul2014	56

The Data Run Identifier is constructed from the short descriptor of the material interrogated and the date on which the run was performed.

5 Analysis

We begin this section with a qualitative discussion of the principal characteristics of the LIF spectra measured against 5HSAS4—a PMC consisting of an epoxy matrix with carbon fabric reinforcement. We then turn to the quantitative analysis used to generate and validate assessment models based on those spectra. Additional subsections describe the analysis of three other PMCs listed in Table 1: BMI, AS4, and 977. All of these spectra were measured using our Gen II Breadboard apparatus with the laser radiant output power set to 5 mW, focused to an irradiation spot covering a roughly circular area slightly larger than 1 cm^2. The collection spot was circular with a diameter of 6 mm, which was determined by transmitting light backward through the collection optics. The irradiation spot was not precisely circular, a consequence of the use of a multi-mode laser; however, it was verified to well-cover the collection spot.

5.1 Qualitative Analysis of the 5HSAS4 Spectra

The 5HSAS4 sample set consists of five SBS specimens for each of nine different sixty-minute temperature treatments ranging from 350° to 510°F, plus an additional five *baseline* (i.e. control) non-baked specimens—50 specimens in all.

The top plot in Figure 6 shows the three spectra measured against specimen B1 on 2 June 2014. One perceives that they have the same general shape, but they differ considerably in intensity. This is no surprise, as these spectra were measured against three different collection spots on the specimen, and at each spot there will be a different fraction of epoxy matrix obscured by the reinforcing fibers. The bottom plot shows that when these spectra are *normalized* by accumulating the intensities of all points between two limits and then dividing all intensities by that sum, they plot virtually on top of each other. This well-illustrates

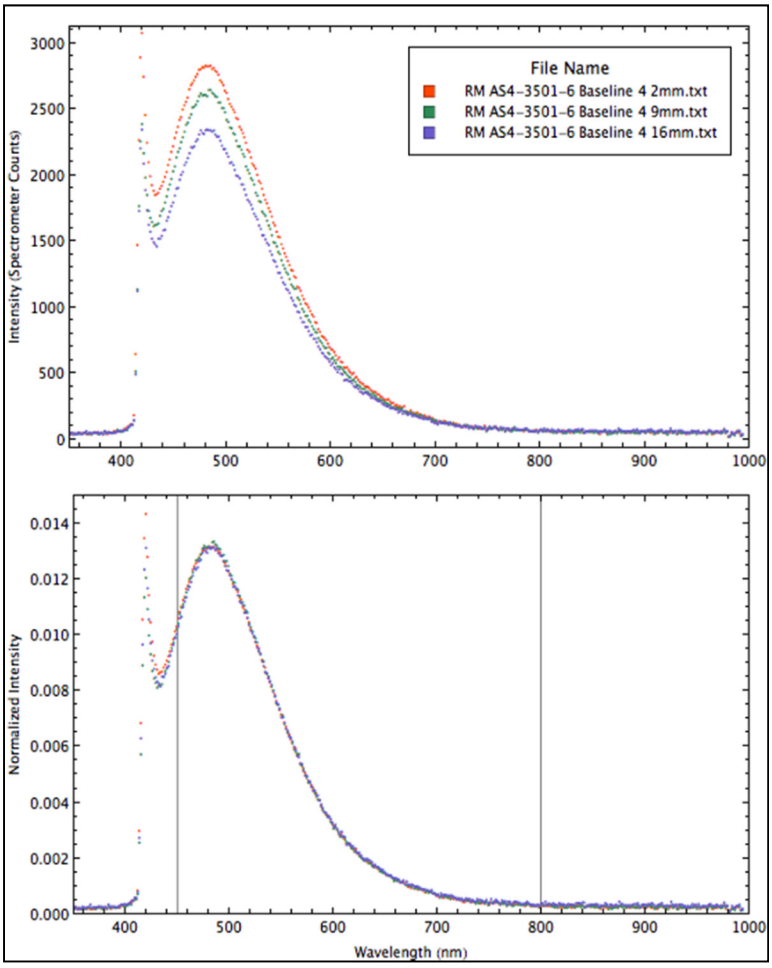

Figure 6. The Effect of Normalization applied to three fluorescence spectra taken against the same specimen of 5HSAS4, showing how absolute intensity can vary at different locations on the specimen while normalized intensity is essentially invariant.

the reason for normalization as the first step of our preprocessing methodology, as described below. In general, spectra taken against the uni-tape-reinforced sample sets will show less intensity variability than those taken against those reinforced by fabric due to the presence of resin pockets in the latter (Meilunas, 2015).

Figure 7 plots one spectrum from each temperature treatment, revealing several trends. First, there is a tendency for the spectra to shift toward longer wavelengths with increasing temperature; second, the absolute intensity tends to increase for higher treatment temperatures. These tendencies were noted by the ORNL group (c.f. Frame *et al.*, 1995, p. 1227), who also showed that fluorescence intensity eventually falls back to well-below that of the undamaged specimens at yet higher treatment temperatures. One should obviously not expect success from an attempt to develop a correlation algorithm based on intensity variation alone, considering that at some level of heat exposure, a significantly damaged material will fluoresce at the same intensity as the un-damaged material.

Another couple of tendencies are worth noting. The skewness (the aforementioned asymmetry of the change of intensity with wavelength to the right of the peak as compared with the left) and the kurtosis (the "peakedness") of the spectra both decrease with increasing treatment temperature.

All of the aforementioned readily discernable changes in spectral features bode well for an attempt to develop an algorithm to correlate incipient heat damage with fluorescence spectra.

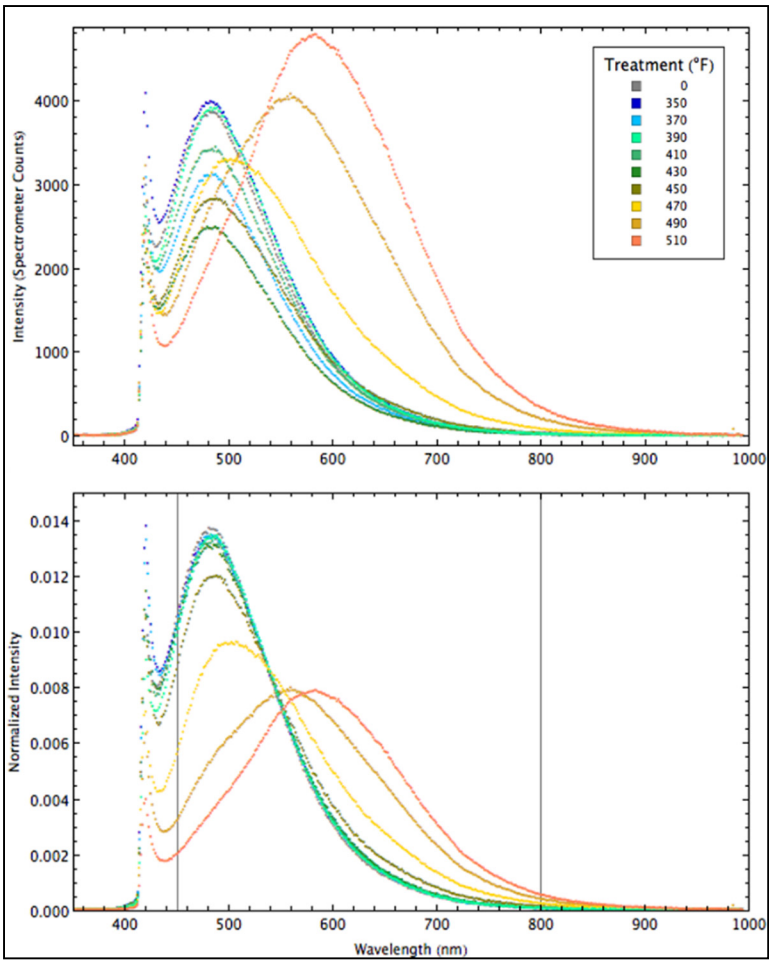

Figure 7. Treatment Temperature Effect on 5HSAS4 Spectra. The progressively increasing peak wavelength and decreasing skewness and kurtosis are clearly evident in the normalized plot (bottom).

5.2 Quantitative Analysis of the 5HSAS4 Spectra

We relied on the excellent book by Beebe *et al.* (1998) for guidance in developing our analysis methodology. The authors define *Chemometrics* as any application of mathematical and statistical techniques to the analysis of chemical data, encompassing preprocessing of the data, through generation of assessment models employing mathematical-statistical algorithms, to validation of such models. Although effective chemometric packages having various degrees of methodological complexity and flexibility are widely available as stand-alone software systems or incorporated into larger systems for spectroscopic analysis or general-purpose mathematical processing, we opted to develop our own methodology and code our own algorithms in the general-purpose mathematical computational system *Mathematica*®. We thereby enjoyed visibility into the intermediate mathematical steps, which yielded valuable insight into the problem. Our analysis methodology is described below in reference to the 5HSAS4 spectra, and that description is also applicable to the other three materials listed in Table 1.

5.2.1 Preprocessing

Preprocessing includes all the steps applied to raw data to prepare the inputs for the mathematical-statistical pattern analysis and correlation algorithms used to generate an assessment model. Descriptions of those steps follows:

5.2.1.1 Normalization

Normalization was introduced above in order to explain the important fact, illustrated in Figure 6, that *normalizing the spectra by setting to unity the area under the spectral curve between reasonably-chosen bounds eliminates most of the variability in spectra measured against the same material subjected to the same thermal treatment*. This effect is so pronounced that, as discussed below, we have found it to provide the primary indicator of whether a given spectrum may have been altered by fluorescence from a contaminant. The specific choice of those bounds—which we call the *normalization limits*—appears not to be critical so long as the lower bound is set to a wavelength slightly longer than that of the local minimum that occurs past the irradiation peak, while the upper bound is set in the tail region well past the wavelengths in which the peak values occur. For internal consistency of the model derivation to follow, the same normalization limits should be applied to all spectra included in any given analysis run.

Mathematically, our normalization algorithm can be specified as follows: Regarding a spectrum S as a list of 1024 intensities s_i corresponding to the list W of wavelengths w_i, i running from 1 to 1024, we compute the *normalization factor*

$$f = {}^{1}\Big/_{\sum_{i=iNmin}^{i=iNmax} s_i}$$

which is then applied to the entire spectrum to derive the *normalized spectrum* N.

$$N = fS$$

Obviously, one calculates unity by summing the normalized spectrum between the *normalization indices* $iNmin$ and $iNmax$. In general, the entire normalized spectrum will sum to a value exceeding unity. (It would sum to unity were the normalization limits set to encompass the entire spectral range.)

For the 5HSAS4 data and all other analyses treated in this report, we set the normalization limits to 450-800 nm; that range encompasses 263 points within the entire 1024-point spectrum, corresponding to a list of 263 wavelengths between 450 and 800 nm.

5.2.1.2 Trimming

Trimming is applied to specify the range of wavelengths used to derive an assessment model from a set of spectra; it is essential that these limits be identical for all spectra in a given analysis run. For the 5HSAS4 data, we set these *analysis limits* to equal the normalization limits, 450-800 nm. Thus, each trimmed spectrum consists of 263 points; in other words, each trimmed spectrum consists of 263 normalized intensity values, corresponding to the list of 263 wavelength values between 450 and 800 nm.

There is no reason why the normalization and analysis limits should necessarily be the same. Our analysis limits were always set to the same values as the normalization limits, so the *analysis indices* $iAmin$ and $iAmax$ were always equal to the *normalization indices* $iNmin$ and $iNmax$, respectively; however, the code allows these limits to be set independently.

5.2.1.3 Culling

Culling is our term for the process of removing certain spectra that show evidence of distortion due to the presence of surface contamination within the interrogation spot. For this study, the set of spectra from each data run were culled using human judgment, comparing spectra from like specimens and looking for disqualifying characteristics. Figure 8 illustrates an example, showing the utility of studying the normalized spectra when judging spectral quality. As is explained in Appendix C, the spectral metadata tables in the data supplement include a column indicating the judged quality of each spectrum, along with a comment giving a reason for each spectrum judged to be inadequate.

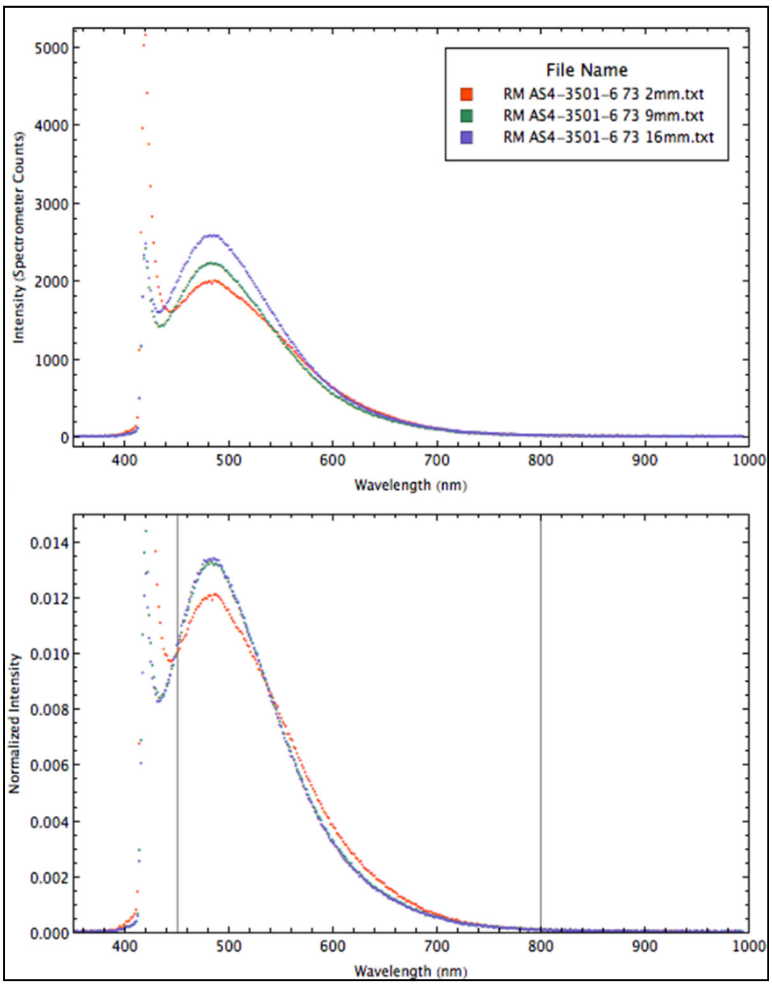

Figure 8. Distortion from Surface Contamination is evident in one of these fluorescence spectra (red trace) taken against the same specimen of 5HSAS4, perhaps from dust or a fingerprint.

Obviously, the follow-on project to develop an automated algorithm will have to devise specific, computationally-implementable criteria to determine whether a given measured spectrum qualifies for analysis, providing a basis to alert the operator of the possibility of surface contamination.

5.2.1.4 Centering

Centering is applied to the set of culled, trimmed spectra to derive the *response matrix R*, which will be processed by mathematical-statistical algorithms to derive an assessment model. This entails summing all the spectra of the set—wavelength for wavelength, then dividing by the number of spectra, and finally subtracting the resulting *centering vector* from all spectra in the set. The response matrix for our 5HSAS4 spectra is plotted in Figure 9, with the trace of each centered spectrum color-coded according to the treatment temperature applied to the specimen against which it was measured. This provides a striking visual representation of how spectral variability correlates to treatment temperature, along with insight into the ranges of wavelength within which the variation is greatest.

For the 5HSAS4 spectra, *R* is a 123×263 element matrix; that is, it consists of 123 rows of normalized, trimmed, centered spectra—each of which has 263 elements, one for each of 263 wavelengths between 450 and 800 nm.

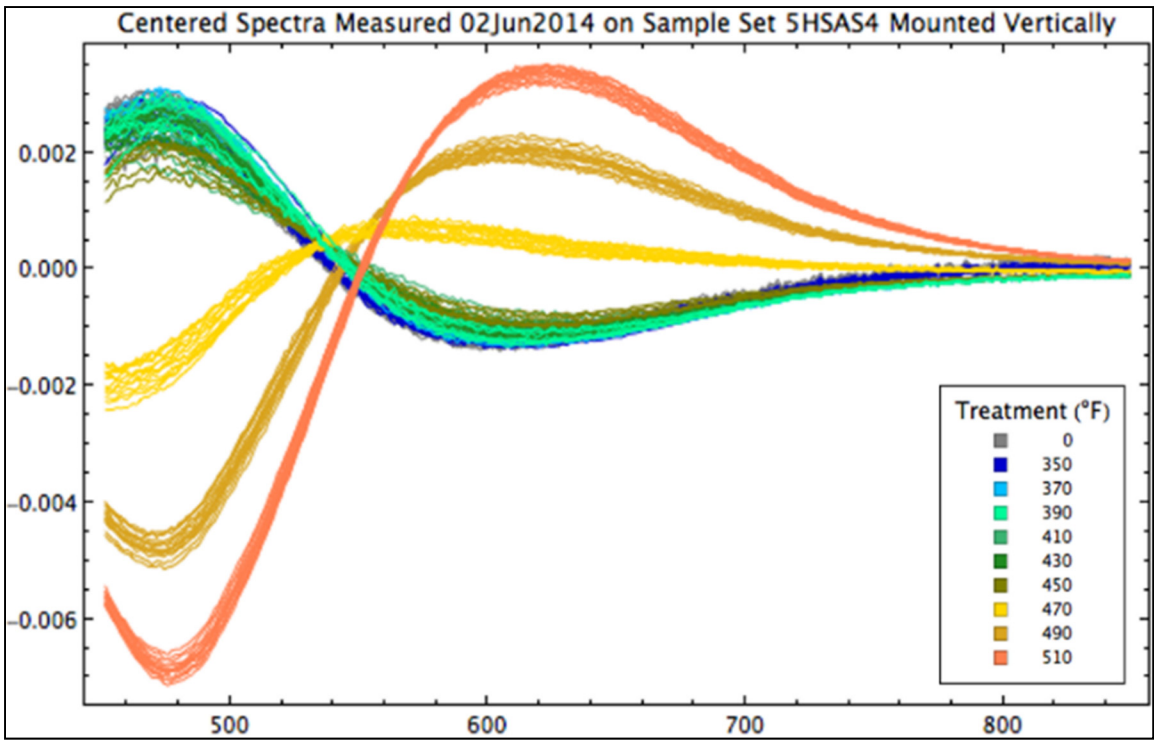

Figure 9. The Response Matrix for 5HSAS4, here represented graphically, was constructed by centering the normalized, trimmed, culled spectra measured on 2 June 2014. Note how the traces for the higher treatment temperatures separate into bands.

5.2.2 Model Generation.

Having derived the response matrix, the next step is to generate an assessment model. Of the various mathematical-statistical analysis procedures that have been devised, the method of *principal components regression* (PCR) was selected—which necessitates the preliminary step of performing a *principal components analysis* (PCA).

5.2.2.1 Principal Components Analysis

PCA is the widely employed algorithm that treats the m rows of an $m \times n$ matrix as points in an n-dimensional Euclidian space: it generates a linear transformation that yields an orthonormal basis set of Cartesian *principal coordinates* (PCs), for which the first coordinate encompasses the greatest variability in the data, the second coordinate encompasses the greatest of the remaining variability, and so on. The total number of PCs is the smaller of m or n, so in our case there are 123 PCs. One typically finds that after a small fraction of the entire set of PCs, the variability encompassed by the next PC is so small as to represent little more than a tiny portion of the residual measurement noise—which, in its totality, can nevertheless amount to a large fraction of the total variability. Where one draws the line to truncate the complete series of PCs is a matter of experimentation and judgment; we have found that nine principal components is a good default for our data.

The PCA algorithm *decomposes* (represents as a product) the response matrix R into the following three matrices:

- The orthonormal *Loading Matrix* V, which has nine columns (one for each principal component) that can be applied to a trimmed, centered spectrum to derive its representation in terms of the first nine principal components. Each column has 263 elements, one element for each wavelength within the analysis limits.
- The orthonormal *Score Matrix* U, for which each of the 123 rows of R is represented by a nine-element row of principal components.
- The diagonal *Singular Value Matrix* S, for which the value of each diagonal element is the fraction of the total variability of R that is encompassed by the respective principal coordinate.

The response matrix can be *recovered* (calculated to within a close approximation) from these three matrices by

$$R = USV^T$$

where the superscript on V indicates that the matrix is to be transposed. By using only the first nine principal components, we do not recover R *precisely*; however, differences from the original will be insignificant ("in the noise") provided enough principal components are used. As previously stated, nine has proved to be sufficient for our data.

Neither the score matrix U nor the loading matrix V lend themselves to an easily understood visual presentation, but it is instructive to examine a pie chart of the diagonal elements of the singular value matrix S. Each segment ("slice") in Figure 10 represents the fraction of the variability in R that is *explained* (as is said) by the respective principal component—by which is meant that a given fraction of the total variability is attributable to variation along that principal coordinate. One can see that the first principal coordinate *alone*

explains about three fourths of the total variability, and that the significance of successive principal components diminishes rapidly. There remains a large residual, which is mostly attributable to measurement noise. (The residual is represented as a single segment in Figure 10, although in fact it consists of segments 10 through 123.)

Beebe et al. (1989, pp. 81-112) provides an excellent intuitive explanation of the PCR algorithm and examples of how it is applied and used to gain insight into the data sets to which it is applied. They cite references where one can find its complete mathematical description and examples of its application in many problem domains.

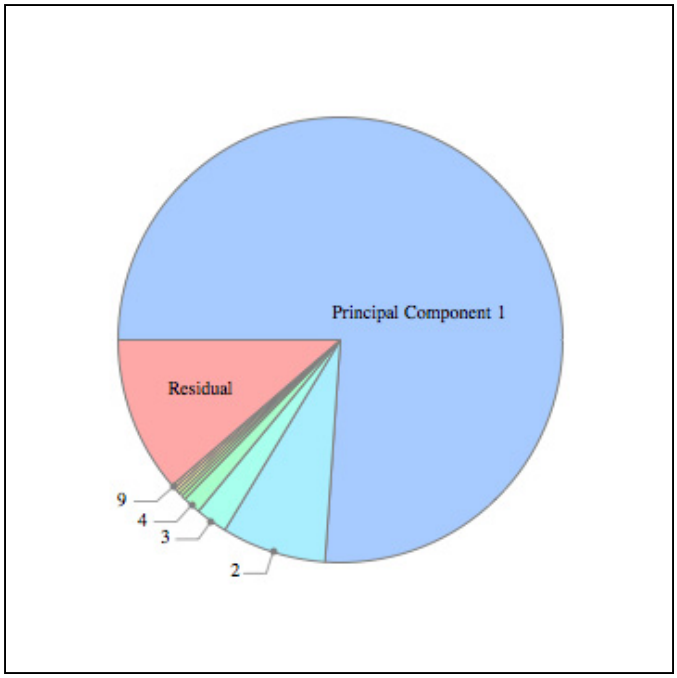

Figure 10. Significance of the Nine Principal Components from the Principal Components Analysis of the 5HSAS4 Response Matrix shown in Figure 9**.**

5.2.2.2 Principal Components Regression

PCR is then used to derive an assessment model in the basis set of the principal components. Conceptually, PCR is simply a particular application of the well-known method of *multiple linear regression* (MLR) to derive the (in our case) nine *regression coefficients* relating the nine principal components to the measured strength data—i.e. the average SBS values.

But the orthonormality of the matrices U and V obviates the need to employ a general MLR algorithm. After *Beebe et al* (1998, pp 280-282), the following steps are taken to generate a predictive model:

- Compute the mean of the SBS values of the specimens against which the (in this case) 123 spectra were taken.
- Subtract the SBS mean value from the aforementioned individual SBS values. Those *centered SBS values* are organized into the 123-element column vector C.
- We then exploit the orthonormal property of the score matrix U to compute the nine-element column vector B of centered regression coefficients β_i:

$$B = U^T C$$

At this point, we have derived the regression coefficients needed to estimate the SBS value of a specimen based on a spectrum measured against it. Before proceeding to describe how we validate the efficacy of our model, it is worthwhile to examine how well the model

performs against the data used to derive it. Letting C^* represent the column vector of 123 *estimated* centered SBS values, we compute

$$C^* = UB$$

from which we then compute the *variance of the fit*

$$\sigma^2 = \sum_{i=1}^{n_s}(c_i - c_i^*)^2 \Big/ n_s$$

and the *standard deviation of the fit* $\sigma = \sqrt{\sigma^2}$, where n_s is the number of spectra—123 in this case.

Remembering to add the mean SBS value to C^* and C to get the estimated and measured SBS values, we can construct a plot to show how well the model performs against the data from which it was constructed. In Figure 11 we plot the estimated vs measured values and include color coding to show how the strength data (SBS values) relate to the respective treatment temperatures. Each spectrum used in the analysis is represented by a point on this plot. The fact that the points for each treatment temperature stack into a vertical column merely reflects the fact that the strength data were given as an *average* value for each given treatment temperature. One would expect a certain amount of horizontal scatter (and a better fit to the data) had the regression been performed against the SBS values of each individual specimen—something that would only be possible for those sample sets consisting of individual SBS specimens (as described above under Material Samples).

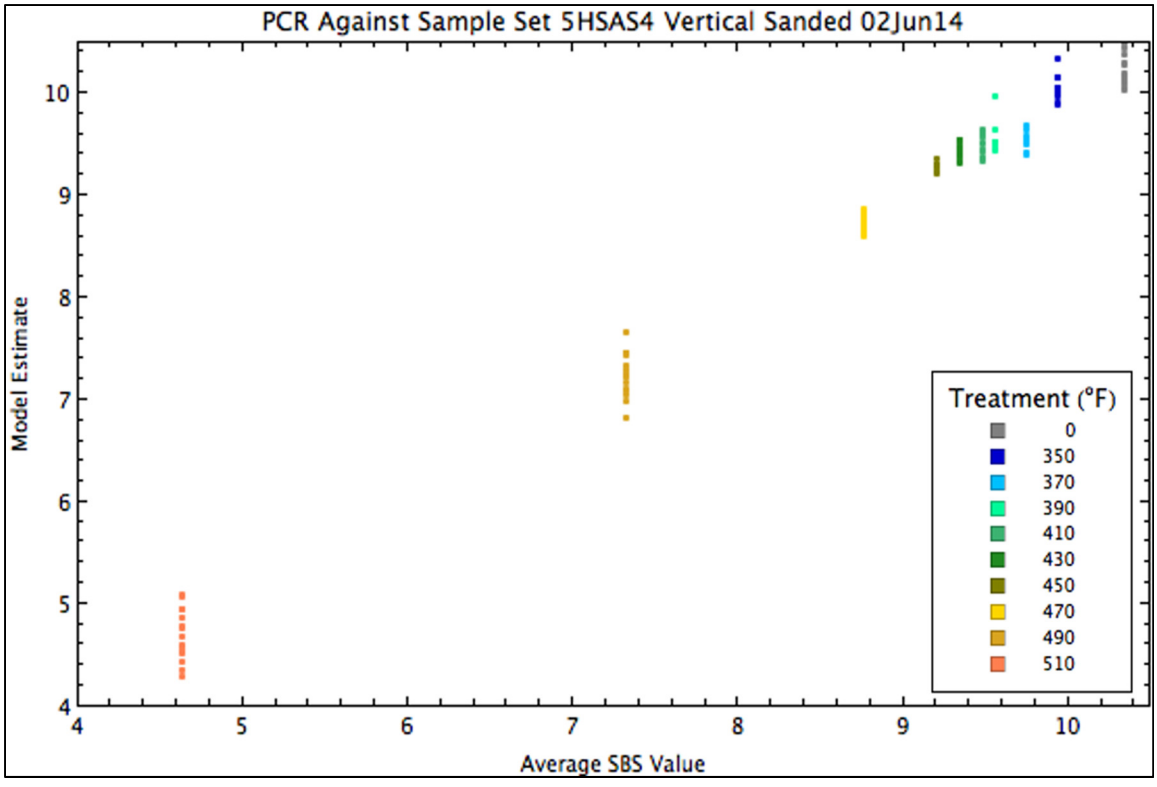

Figure 11. The Model Fit to 5HSAS4 Spectra is here illustrated graphically. Each qualified spectrum measured on 2 June 2014 is represented by a point on this plot. The spread of the vertical columns indicates the variability in the model estimate of the average SBS value for each treatment temperature.

5.2.3 Validation.

Validation of an assessment model is performed by testing it against data that were *not* used in its construction. Two approaches were considered:

1. *Random Partitioning.* One can randomly partition the spectra from a given data run into two independent sets: The *Training Set*—to be used to generate an assessment model, and the *Validation Set*—to be used to test the efficacy of that assessment model. This is the procedure used for all validations discussed in this report.

2. *Independent Data Sets.* We took two independent data runs against 5HSAS4 (i.e. spectra were measured against all specimens on two different days); hence, we could declare the entirety of data from one run to constitute the training set and the other run to constitute the validation set. To employ that approach, one must account for systematic drift in the spectrometer's response in both wavelength and intensity—which would introduce complexities that fall beyond the scope of this study. The follow-on effort to develop the Gen II Prototype will need to incorporate the ability to correct for spectrometer drift, for which a number of well-known calibration methods can be brought to bear.

For validation of both of the two 5HSAS4 data runs (and all other data runs reported herein), a partitioning generator was developed that employs a pseudorandom number generator to select a training set consisting of 60% of the spectra, with the remaining 40% consigned to the validation set. To ensure reproducibility of each analysis run, specific integer-denoted *random streams* were defined with reference to a *Base Random Stream* determined by a specific random seed setting of a specific *Mathematica*® pseudorandom generator. For the 2 June 2014 data run, Figure 12 shows that the model correctly separated all spectra of the validation set according to whether or not they were assessed to retain at least 80% of their strength—which was established at the beginning of the project as the objective. Figure 13 shows similar success for the 6 June data run. These, and all subsequent validation charts are divided into four quadrants. The vertical division line separates the specimens into those that have retained at least 80% of their strength *by actual measurement*, while the horizontal division line separates them according to the same criterion *as estimated by the assessment model*. To add clarity, a check symbol (✔) is used to denote that the spectrum has *passed* by the aforementioned 80%-strength criterion, while a crossout symbol (✘) denotes failure by that criterion. In the jargon of validation, there are four possible outcomes of a model evaluation applied to any spectrum:

- **True Positive**, indicated by a check (✔) in the upper-right quadrant
- **False Positive**, indicated by a check (✔) in the upper-left quadrant
- **True Negative**, indicated by a crossout (✘) in the lower-left quadrant
- **False Negative**, indicated by a crossout (✘) in the lower-right quadrant

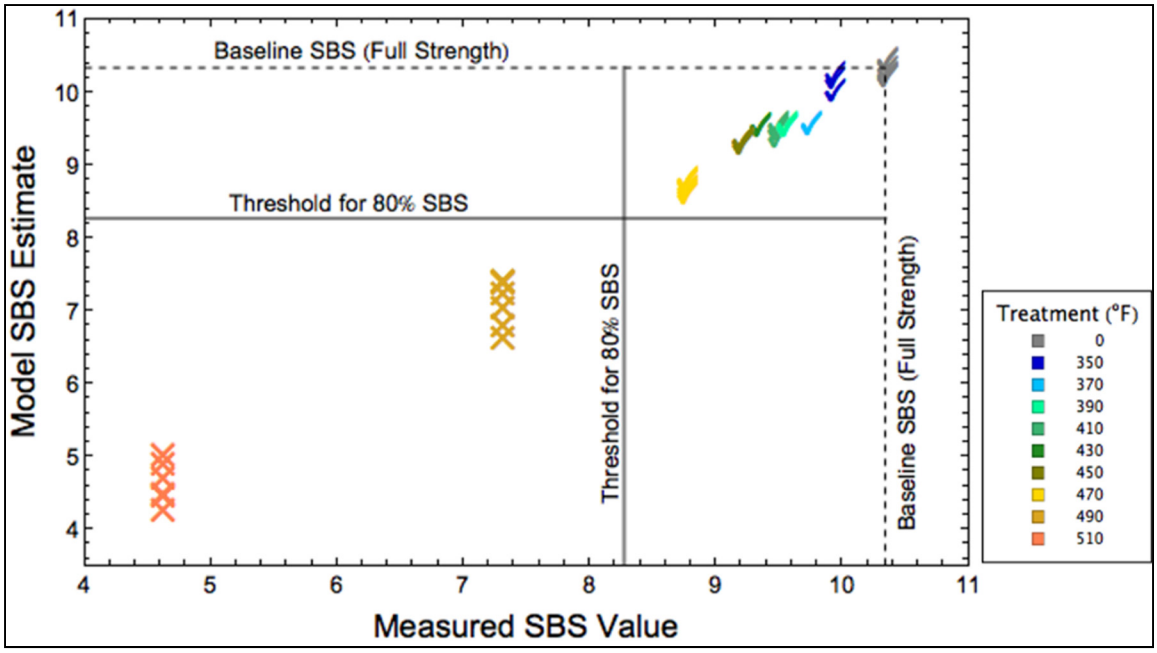

Figure 12. Validation Chart for 5HSAS4 Spectra Measured 2 June 2014. This is similar to the model fit chart (Figure 11), but here the 5HSAS4 spectra were gathered by random partitioning into independent training and validation sets using the Base Random Stream. The training set was used to construct the model that was then used to classify the validation set, yielding the results shown in this chart.

While hopefully adding clarity, this use of check and crossout symbols along with the horizontal division line is redundant: *Every* spectrum assessed *by the model* to pass is represented by ✔ appearing *above* the division line; likewise, *every* spectrum assessed by the model to fail the criterion is represented by ✕ appearing *below* the division line.

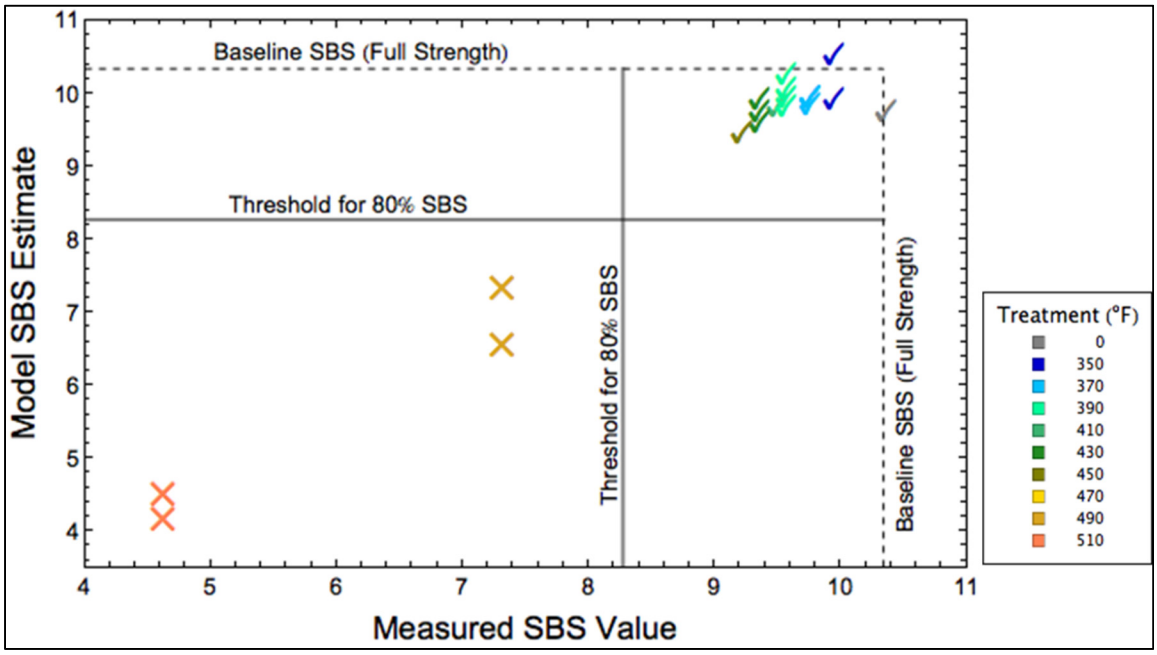

Figure 13. Validation Chart for 5HSAS4 Spectra Measured 6 June 2014, partitioned using Random Stream 9**.**

In viewing these two validation charts, the reader is cautioned not to take the lack of false negatives and false positives to ascribe perfection to our simple assessment modeling methodology. There is little doubt that by repeating the analyses of either of these two 5HSAS4 data sets enough times using different random streams, we would encounter instances of false outcomes. In the follow-on effort to develop a fieldable system, we would assess the statistical performance of our current modeling methodology as a baseline, devise enhancements to minimize the occurrence of false outcomes, and develop indicators to alert the operator in cases of high uncertainty.

That said, an informal check of our modeling methodology was performed by trying about ten different random streams, none of which yielded a single false-positive or false-negative assessment. Note that this was *not* an exhaustive search.

5.3 Analysis of the BMI Spectra

The detailed, step-by-step explanation of how the 5HSAS4 spectra were analyzed need not be repeated for the other three materials treated in this report. In this section, we show that BMI lives up to its reputation of having a higher thermal operating range: there is much less susceptibility to heat damage at any given temperature in comparison with 5HSAS4. Despite being taken to higher temperatures, we see in Figure 14 that BMI exhibits a great deal more variation in intensity with increasing treatment temperature compared to 5HSAS4; there is far less variation in frequency, however. The response matrix for BMI, Figure 15, shows that the normalized intensity varies with frequency by about a tenth of what is observed for 5HSAS4 (Figure 9).

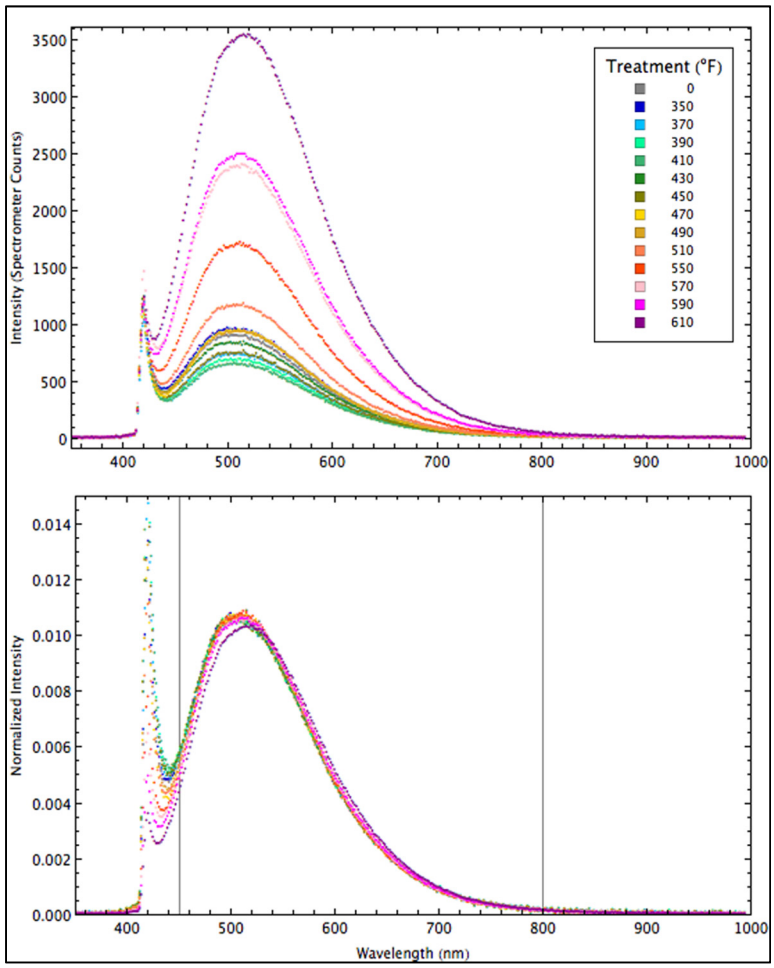

Figure 14. Treatment Temperature Effect on BMI Spectra. Compared with 5HSAS4 (Figure 7), the increase of intensity with treatment temperature is much more pronounced, while the frequency shift is much smaller.

Nevertheless, the validation chart for the BMI spectra from 29 May (Figure 16) shows that the chemometric analysis code we developed can generate assessment models from the BMI spectra—in this instance

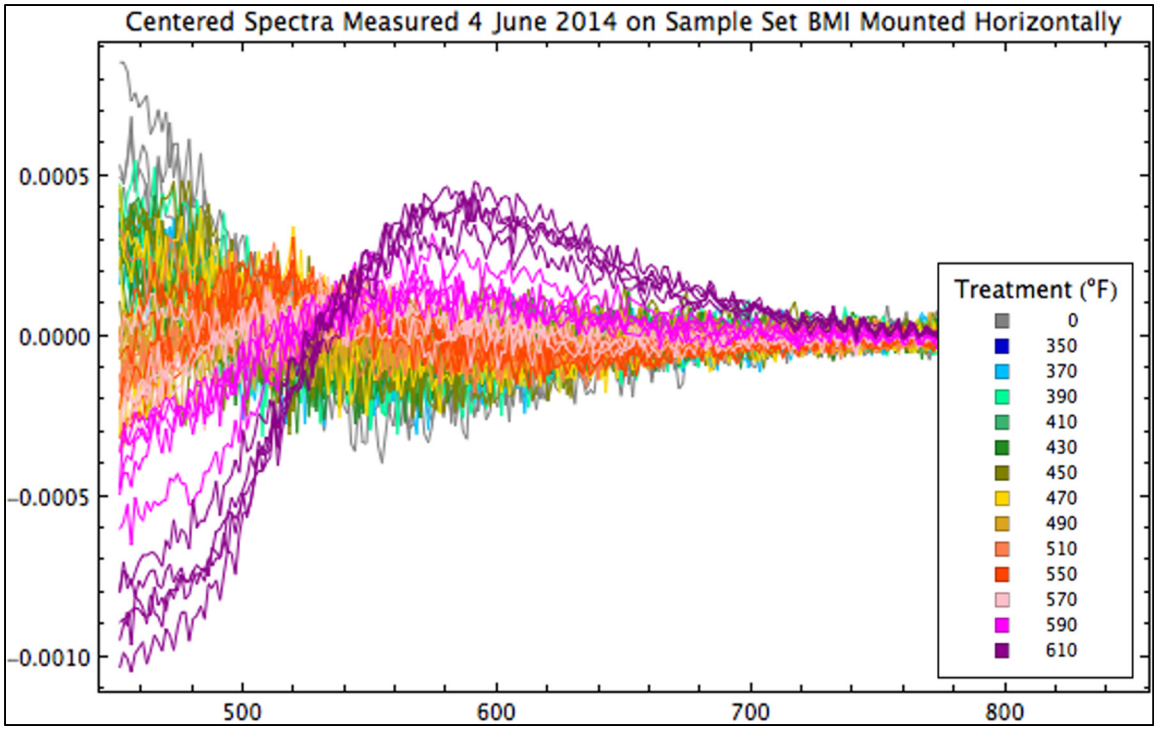

Figure 15. Response Matrix for BMI Spectra Measured 4 June 4 2014. These variations are an order of magnitude smaller than those for 5HSAS4 (Figure 9).

yielding one false-positive assessment. False assessments occur more readily when analyzing BMI spectra, which is understandable in view of the smaller variations across treatment temperature that the modeling code has to work with. Figure 17 shows the validation chart for the BMI spectra taken on 29-30 May, showing two false-positive assessments.

It is tempting to wonder if one might construct a more effective analysis methodology for BMI if intensity trends could be taken into account. Considering that normalization was introduced in order to cope with the large variations in fluorescence intensity that arise from spot to spot on the same specimen, it would be necessary to account for the variation in the fraction of matrix material vs carbon fiber exposed to radiation in order to include the effect of intensity variations without introducing ambiguity into the correlation exercise. No simple means to achieve that is apparent to us, and the fact that our (quite basic) analysis algorithm yields promising results suggests to us that the best path toward improved performance lies in exploring the many tools of chemometrics that can be brought to bear to better analyze the shape of normalized spectra—even though that approach entails ignoring the intensity effect. This question could be revisited as part of the follow-on effort to develop a field-portable system.

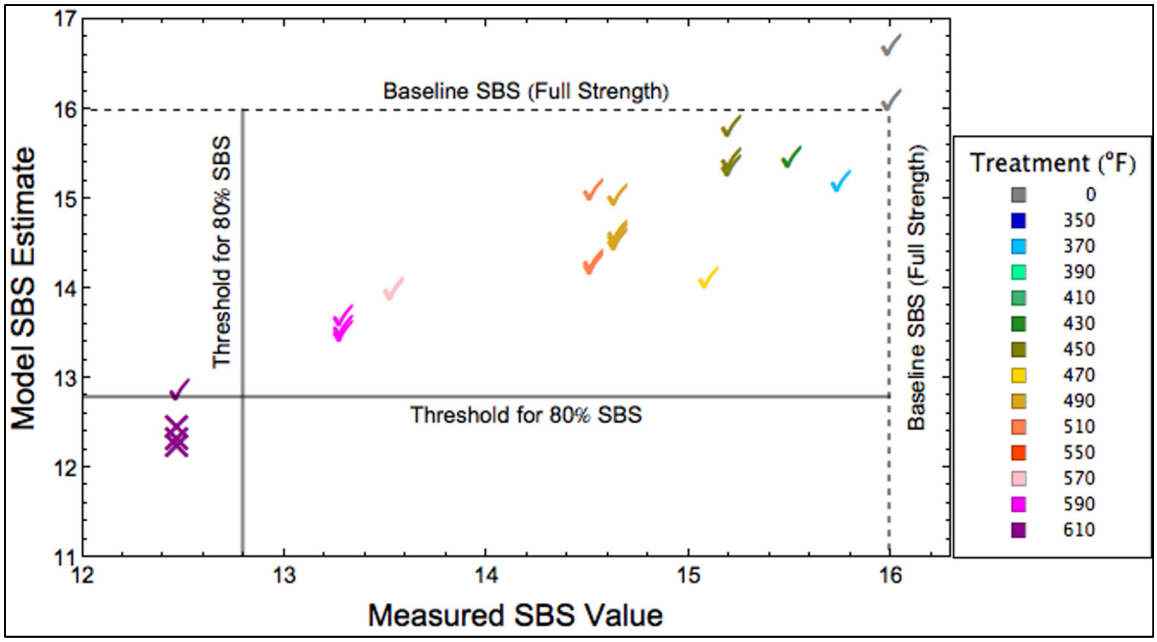

Figure 16. Validation Chart for BMI Spectra Measured 4 June 2014, partitioned using Random Stream 15. Note the occurrence of one false-positive response.

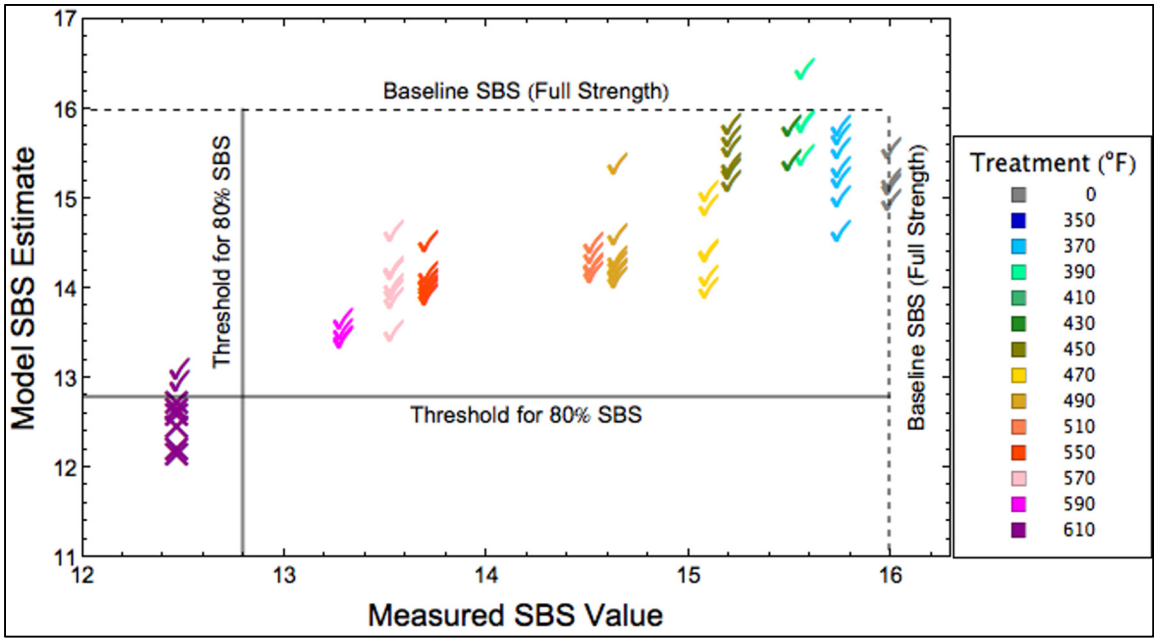

Figure 17. Validation Chart for BMI Spectra Measured 29-30 May 2014, partitioned using Random Stream 4. Note the occurrence of two false-positive responses.

5.4 Analysis of the AS4 and 977 Spectra

Figures 18 and 19 show the response matrix and validation chart for AS4 (our short descriptor for AS4/3501-6 Uni-Tape), and Figures 20 and 21 show the response matrix and validation chart for 977 (short for IM7/977-3 Uni-Tape). The behavior of the AS4 and 977 materials is similar to that of 5HSAS4, which is understandable considering their similar makeup. AS4 differs from 5HSAS4 only in that unidirectional AS4 carbon fiber is used instead of AS4 carbon fabric as the reinforcing material. Both materials contain the same epoxy matrix, 3501-6, from which the fluorescence originates. Though 977 is considered a "toughened" resin due to the addition of a thermoplastic toughened phase to the epoxy that forms the matrix (CYCOM® 977-3 Technical Data Sheet), the LIF response is similar to 3501-6 epoxy.

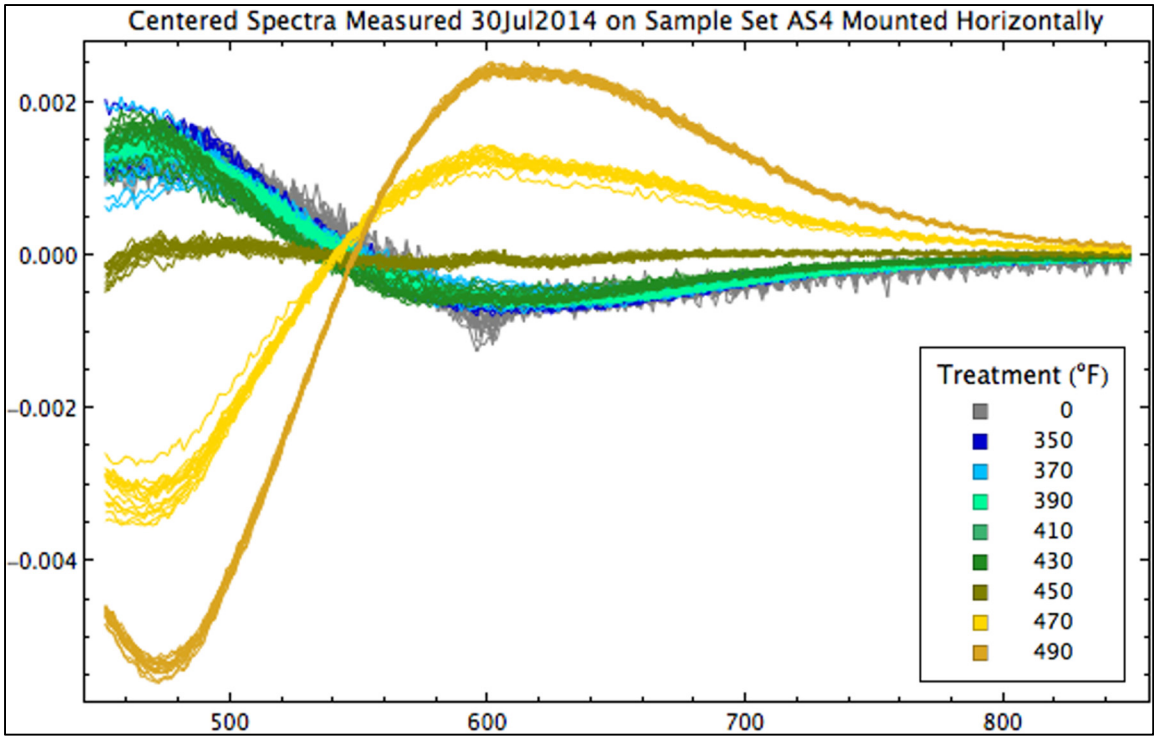

Figure 18. Response Matrix for AS4.

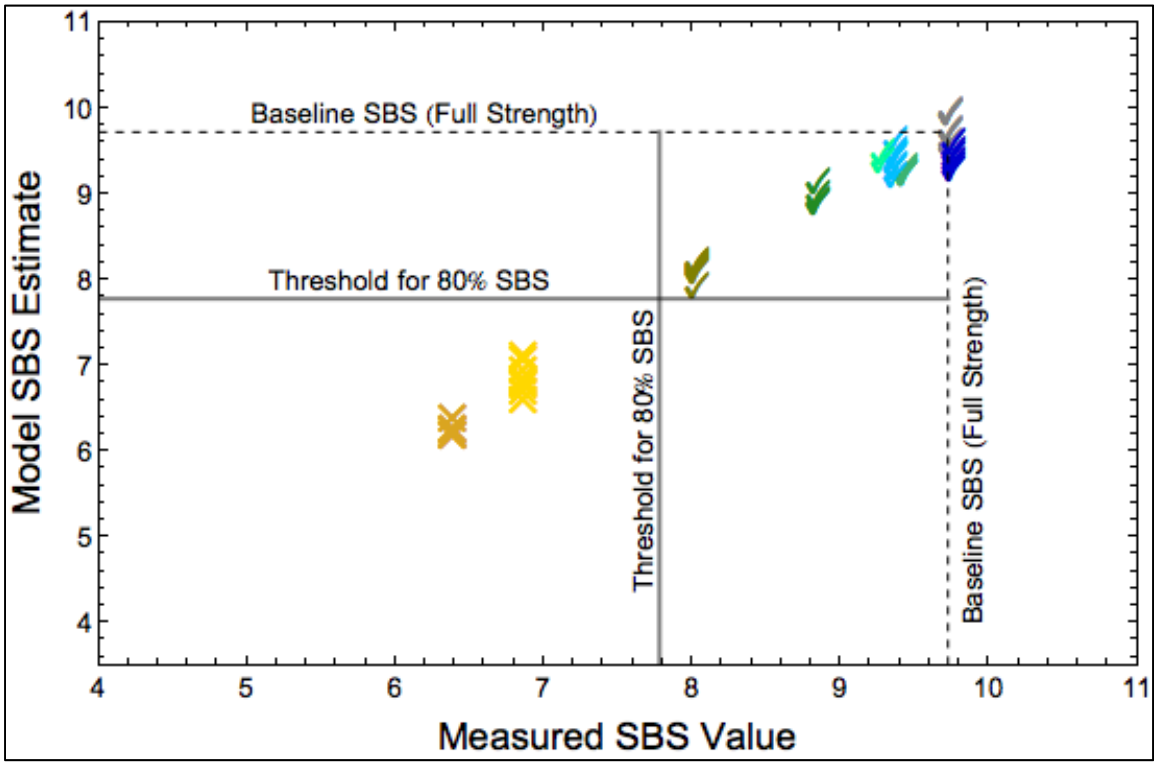

Figure 19. Validation Chart for AS4, partitioned using the Base Random Stream.

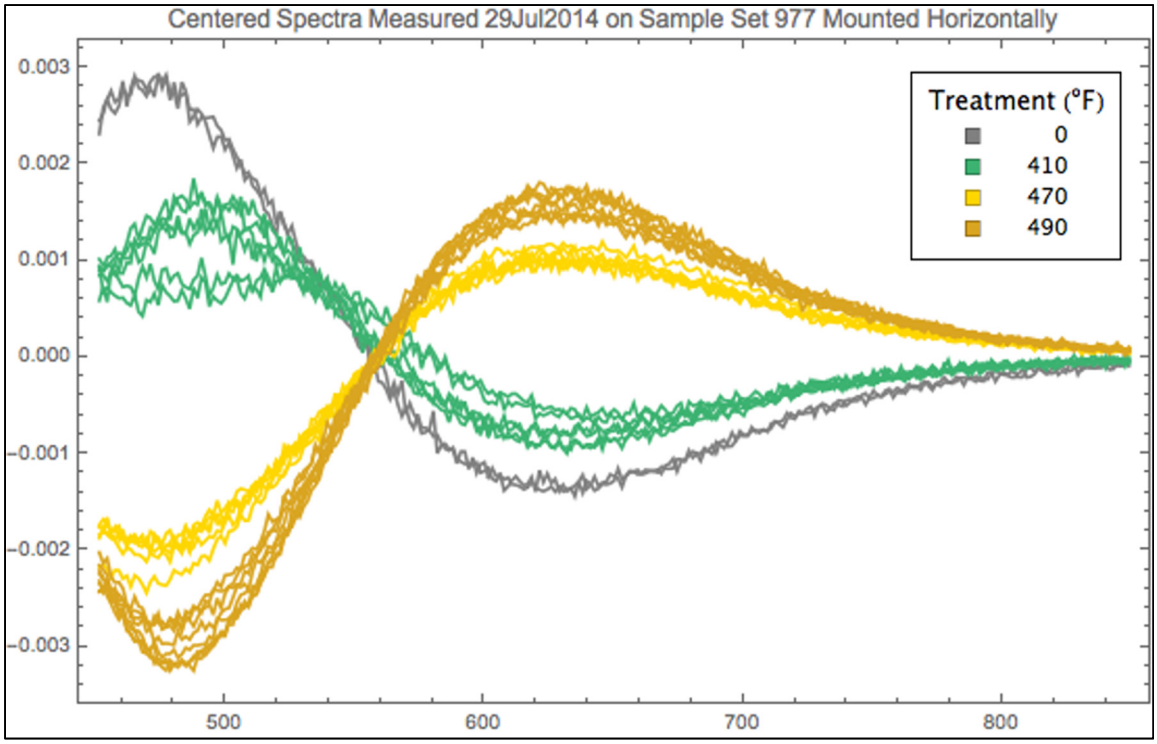

Figure 20. Response Matrix for 977.

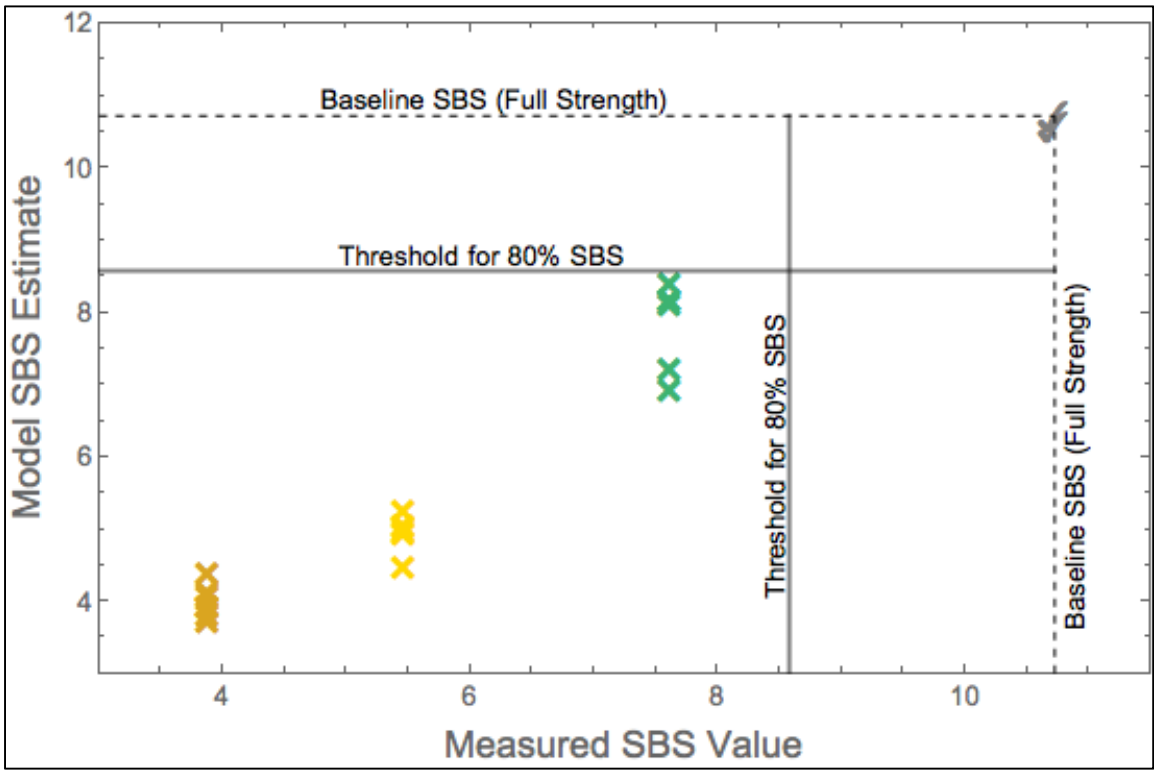

Figure 21. Validation Chart for 977, partitioned using the Base Random Stream.

6 Conclusion

We have demonstrated that a laboratory apparatus, assembled from COTS components that were not structurally modified in any way, can measure fluorescence data that can be analyzed to assess whether any of four different composite materials have experienced incipient heat damage sufficient to degrade their structural strength, according to the SBS standard, to less than 80% of that of the undamaged material. The efficacy of our Gen II Breadboard apparatus and associated chemometric analysis software was demonstrated against three materials in the epoxy-matrix family and one in the BMI-matrix family. Thus, we have successfully concluded the first phase of this effort.

We submit that proceeding to the follow-on project to design and fabricate a fieldable Gen II Prototype is warranted. The Gen II Prototype development effort will need to address the following issues, among others:

- **Data.** A great deal of data is required to develop an assessment modeling methodology that can pass the verification and validation requirements for operational implementation. Besides expanding the list of materials to include all that are operationally significant, it will be necessary to account for such real-world considerations as the facts that some degree of degradation develops from normal operations ("aged" materials), and that degradation under a given heat load can be aggravated if the material is saturated with water (Browning *et al.*, 1977).

- **Packaging.** The laser, irradiation optics, collection optics, and spectrometer will need to be mounted in a shock-resistant, human-portable unit that includes a power supply.

- **Optics.** The optics should permit interrogation of the tested surface through a handheld probe, as is the case with the current Gen I Prototype. There should be a capability to select any of several different probes to facilitate interrogation of surfaces in different arrangements, to include wide, flat or gently curved surfaces such as wings as well as narrow or angled crevices. Probe requirements should be addressed early in collaboration with the user community.

- **Calibration.** Means for built-in calibration must be devised to correct for the drift in wavelength and intensity response—an inevitable characteristic of all spectrometers.

- **Automated Data Quality Assessment.** An algorithm should be developed to examine a spectrum for distortions characteristic of contamination by some foreign fluorescent substance, such as dust or oil. The operator should be alerted when a given spectrum fails to pass this quality test, and such spectra should be eliminated from the chemometric analysis so as to reduce false-negative and false-positive readings.

Intentionally Blank

7 References

ANSI Z136.1–2007. *American National Standard for Safe Use of Lasers*, ANSI Z136.1-2007, Laser Institute of America, p. 19, approved March 16, 2007 by American National Standards Institute, Inc.

ASTM D2344, 2013. *Standard Test Method for Short-Beam Strength of Polymer Matrix Composite Materials and Their Laminates*, ASTM International, West Conshohocken PA.

Beebe *et al.*, 1998. Kenneth R. Beebe, Randy J. Pell, & Mary Beth Seacholtz, *Chemometrics: A Practical Guide*, John Wiley & Sons, Inc.

Bowie, 2017. Christopher M. Bowie, Master's thesis, The Pennsylvania State University, to be published.

Browning, *et al.*, 1977. C. E. Browning, et. al., *Moisture Effects in Epoxy Matrix Composites*, Air Force Materials Laboratory technical report AFML-TR-77-17.

CYCOM 5250-4 Tech Data Sheet. Technical Data Sheet for CYCOM® 5250-4 Prepreg System, Cytec Industries Incorporated, posted at https://cytec.com/sites/default/files/datasheets/CYCOM_5250-4_032012.pdf.

CYCOM 977-3 Tech Data Sheet. Technical Data Sheet for CYCOM® 977-3 Epoxy Resin System, Cytec Industries Incorporated, posted at http://cytec.com/sites/default/files/datasheets/CYCOM_977_3.pdf.

Fisher *et al.*, 1995. W. G. Fisher, et. al., "Nondestructive Inspection of Graphite-Epoxy Composites for Heat Damage Using Laser-Induced Fluorescence," *Applied Spectroscopy* **49** (9), 1225-1231.

Fisher *et al.*, 1997. W. G. Fisher, et. al., "Laser Induced Fluorescence Imaging of Thermal Damage in Polymer Matrix Composites," *Materials Evaluation/June 1997*, 726-729.

Frame *et al.*, 1990. B. J. Frame, et. al., *Composite Heat Damage, Part 1. Mechanical Testing of IM6/3501-6 Laminates, Part 2. Nondestructive Evaluation Studies of IM6/3501-6 Laminates*, ORNL/ATD-33, Oak Ridge National Laboratory, Oak Ridge TN.

Haskins, 1989. J. F. Haskins, "THERMAL AGING", *SAMPE J.* **25**, 29.

Hexcel 3501-6 Product Data Sheet. Product Data Sheet for Hexcel® 3501-6 Epoxy Matrix, Hexcel Corporation, posted at http://www.hexcel.com/Resources/DataSheets/Prepreg-Data-Sheets/3501-6_eu.pdf.

HexTow AS4 Product Data Sheet. Product Data Sheet for HexTow® AS4 Carbon Fiber, Hexcel Corporation, posted at http://www.hexcel.com/Resources/DataSheets/Carbon-Fiber-Data-Sheets/AS4.pdf.

HexTow IM7 Product Data Sheet. Product Data Sheet for HexTow® IM7 Carbon Fiber, Hexcel Corporation, posted at http://www.hexcel.com/Resources/DataSheets/Carbon-Fiber-Data-Sheets/IM7.pdf.

Janke *et al.*, 1990. C. J. Janke, et. al., *Composite Heat Damage Spectroscopic Analysis*, ORNL/ATD-42, Oak Ridge National Laboratory, Oak Ridge TN.

Kerr & Haskins, 1984. J. R. Kerr & J. F. Haskins, "Effects of 50,000 h of Thermal Aging on Graphite/Epoxy and Graphite/Polyimide Composites," *AIAA Journal* **22**, 96-102.

Kerr & Haskins, 1987. *Time-Temperature-Stress Capabilities of Composite Materials for Advanced Supersonic Technology Application*, NASA Contractor Report 178272.

Luoma & Rowland, 1986. G. A. Luoma & R. D. Rowland, "Environmental Degradation of an Epoxy Resin Matrix," *Journal of Polymer Science* **32**, 5777-5790.

Matzkanin & Hansen, 1998. George A. Matzkanin and George P. Hansen, *Heat Damage in Graphite Epoxy Composites: Degradation, Measurement and Detection*, A State-of-the-Art Report for the Nondestructive Testing Information Analysis Center (NTIAC), Document No. NTAIC-SR-98-02, September 1998.

Meilunas 2015. Raymond Meilunas, private communication.

NAVAIR Heat Damage Standards. Interested parties should contact Dr. Raymond Meilunas of the Naval Air Systems Command, Code 4.3.4.4, phone (301) 342-8064, email Raymond.Meilunas@Navy.mil.

R&D 100 Awards, 2008 a. "Aircraft Inspection Keeps Pace with Composite Age," *R&D Magazine* **50** (5), 47, September 2008.

R&D 100 Awards, 2008 b. RDMag.com, 26 September 2008. *Aircraft Inspection Keeps Pace with Composite Age*. [online] Available at http://www.rdmag.com/award-winners/2008/09/aircraft-inspection-keeps-pace-composite-age [Accessed 15 February 2017].

R&D 100 Awards, 2008 c. YouTube.com, July 19, 2009. *Laser-Induced Fluorescence Heat Damage Detector*. [online] Available at https://www.youtube.com/watch?v=lVw9BZF9bEM [Accessed 15 February 2017].

APPENDIX A. Accessing Data on the NAVAIR Composite Heat Damage Standards

The Microsoft Excel workbook *LIF Spectra on NAVAIR Samples*, which is read directly by the *Mathematica*® code developed for this project, is included in the Data Supplement. The image below reproduces the worksheet **SBS_977**, which documents the treatments applied to each of the four specimens comprising sample set 977. The table within the tan background is formatted in a specific manner that permits our code to access the data. This workbook includes the following worksheets of data on the NAVAIR Composite Heat Damage Standards used in this study:

- SBS_AS4 Sample Set AS4: AS4/3501-6 Uni-Tape (Epoxy)
- SBS_BMI Sample Set BMI: IM7/5250-4 Uni-Tape (BMI, Qualified)
- SBS_5HSAS4 Sample Set 5HSAS4: AS4/3501-6 Fabric (Epoxy)
- SBS_977 Sample Set 977: IM7/977-3 Uni-Tape (Toughened Epoxy)

All of these data were provided by Dr. Raymond Meilunas (NAVAIR 4.3.4.4) in labeling and documentation accompanying the sample sets or in separate correspondence.

NAVAIR 4.3.4.4 Sample Set 977: IM7/977-3 Uni-Tape (Toughened Epoxy)

Explanation of Column Headings

Specimen ID	**The specimen's unique identifier.**
Temperature	**The temperature (°F) at which the specimen was baked, or 0 for a control specimen that was not baked.**
Duration	**The duration (min) for which the specimen was baked, or 0 for a control specimen that was not baked.**
SBS	**Value of the short-beam shear (SBS) measurement (ksi) for this specimen, or the average value of a set receiving the same treatment.**

//SBS_977 DD *

NAVAIR 4.3.4.4 Sample Set 977: IM7/977-3 Uni-Tape (Toughened Epoxy)

	SpecimenID	Temperature	Duration	SBS	/*
1	CTRL	0	0	10.723	
2	7617	410	60	7.617	
3	5473	470	60	5.473	
4	3890	490	60	3.890	

/* Data provided by Dr. Raymond Meilunas, NAVAIR 4.3.4.4

Intentionally Blank

APPENDIX B. Example Spectral Data File

Our analysis code inputs spectral data directly from the data files output by the Ocean Optics *SpectraSuite*® software used to control the *QE 65 Pro* spectrometer. An example of those data files, which are in standard tab-delimited text format, is provided below:

```
SpectraSuite Data File
++++++++++++++++++++++++++++++++++
Date: Fri Jun 06 15:58:34 EDT 2014
User: admin
Dark Spectrum Present: Yes
Reference Spectrum Present: No
Number of Sampled Component Spectra: 1
Spectrometers: QEPB0495
Integration Time (usec): 1000000 (QEPB0495)
Spectra Averaged: 1 (QEPB0495)
Boxcar Smoothing: 0 (QEPB0495)
Correct for Electrical Dark: No (QEPB0495)
Strobe/Lamp Enabled: No (QEPB0495)
Correct for Detector Non-linearity: No (QEPB0495)
Correct for Stray Light: No (QEPB0495)
Number of Pixels in Processed Spectrum: 1044
>>>>>Begin Processed Spectral Data<<<<<
198.01     6.00
198.81     5.00
199.61     0.00
200.41     -2.00
... Intermediate spectral points removed
450.58     2079.00
451.36     2122.00
452.14     2140.00
452.92     2168.00
453.69     2192.00
... Intermediate spectral points removed
992.34     -1.00
993.06     -5.00
993.78     -1.00
>>>>>End Processed Spectral Data<<<<<
```

The metadata at the beginning documents the date and the spectrometer settings in effect for the measurement. Each point in the spectrum is specified in a separate line, with the wavelength and intensity specified in that order.

Intentionally Blank

APPENDIX C. Accessing the Spectral Data Measured in this Study

The Microsoft Excel workbook *LIF Spectra on NAVAIR Samples*, which is read directly by the *Mathematica* code developed for this project, is included in the Data Supplement. The image below reproduces a selected portion of table **Spectra_977_29Jul2014** in worksheet **977 Spectra 29Jul2014**, which documents the metadata connecting specimens of sample set 977 with the spectra measured against them during the 29 July 2014 data run. Our analysis code inputs metadata from tables such as this to determine the appropriate data file to input for each spectrum identifier.

//Spectra_977_29Jul2014 DD *					
Spectra Measured 29Jul2014 on Sample Set 977 Mounted Horizontally					
SpectrumID	SpecimenID	FileName	Quality	/*	Comments
1	CTRL	977 ID_CTRL BL S H 1.txt	-		
2	CTRL	977 ID_CTRL BL S H 2.txt	X		Spectrum i
3	CTRL	977 ID_CTRL BL S H 3.txt	-		
… Intermediate rows removed …					
13	7617	977 ID_7617 410F S H 1.txt	-		
14	7617	977 ID_7617 410F S H 2.txt	-		
15	7617	977 ID_7617 410F S H 3.txt	-		
… Intermediate rows removed …					
28	5473	977 ID_5473 470F S H 1.txt	-		
29	5473	977 ID_5473 470F S H 2.txt	-		
30	5473	977 ID_5473 470F S H 3.txt	-		
… Intermediate rows removed …					
42	3890	977 ID_3890 490F S H 1.txt	-		
43	3890	977 ID_3890 490F S H 2.txt	-		
44	3890	977 ID_3890 490F S H 3.txt	-		
… Intermediate rows removed …					
56	3890	977 ID_3890 490F S H 15.txt	-		
/* Data measured 29 July 2014 by Daniel Merdes, Daniel Sills, & Raymond					Meilunas

Text in cells under the **Comments** header are not input by our code, but serve to document our reason for declaring a given spectrum to have poor quality. In the above excerpt, spectrum 2 is marked as having unacceptable quality, and the comment reads in full as follows: "Spectrum is severely misshapen. Suspect contamination."

The workbook includes six worksheets of spectral metadata:

- **BMI Spectra 29May14**
- **5HSAS4 Spectra 02Jun14**
- **BMI Spectra 04Jun14**
- **5HSAS4 Spectra 06Jun14**
- **977 Spectra 29Jul14**
- **AS4 Spectra 30Jul2014**

Intentionally Blank

APPENDIX D. The Data Supplement

All data discussed in this report are included in the accompanying CD. Additional copies are available on request to author Merdes.

This Data Supplement CD has been posted as a zip-file at The Pensylvania State University's ScholarSphere repository and is accessible at https://doi.org/10.18113/S15K5T

Intentionally Blank

APPENDIX E. Irradiation Through Optical Fiber

The open design of the Gen II Breadboard permits variation of experimental conditions to test the efficacy of alternative components (radiation sources, filters, lenses, spectrometers, etc.) and independent adjustment of the spot sizes for irradiation and collection. Specimens of different sizes and shapes can be accommodated because the design places the irradiation and collection optics at a comfortable distance. Having the laser's output directly focused onto the specimen permits accurate measurement of the irradiance applied; however, that design feature could be construed as an artificiality for what we are putting forward as the precursor to a field-portable instrument. A fielded LIF NDE system will have to be able to evaluate the component in question in place on the aircraft in the hangar or airfield environment, pretty much guaranteeing that such an instrument will need to irradiate the structure being tested through an optical fiber cable. (It will also have to transmit the collected fluorescence emission back to the unit through optical fiber, as is already the case in the Gen II Breadboard.) The follow-on study to develop the Gen II Prototype will need to use (perhaps even develop) a probe to irradiate the test object, collect the fluorescence emission, and transmit it back to the spectrometer through optical fiber—as does the Gen I Prototype described in the Background section of this report. While optical fiber does conduct light rather efficiently, there are substantial losses at each interface between fiber and air.

Inasmuch as we are proposing to advance this work to the level of field application, we decided to perform a crude demonstration that one can measure quality spectra with our apparatus while irradiating the source through an optical cable instead of directly through space. As shown in Figure E1, we rigged an available reflectance probe to intercept the laser's output (operated at 5 mW as during our data runs) and irradiated the specimen through the probe's central optical fiber. Figure E2 is a detail showing the probe's input cable for the center fiber mounted to intercept the laser beam—with a collimator affixed to facilitate efficient collection. Figure E3 shows the pattern of the irradiation spot on the specimen. Figure E4 shows plots of spectra, using three different integration times, collected against that spot on the specimen irradiated by the probe, along with a single spectrum measured against the same spot on the same specimen under the same *direct* laser irradiation used in the experimental runs documented by this report. All of the normalized spectra plot virtually on top of each other. This shows that it should be possible to design optical probes to interrogate composite objects, with radiation transmitted to the probe, and fluorescence collected and transmitted from the probe, through optical fiber.

The specimen was a piece of AS4/3501-6 5HS, a Fabric-Reinforced Epoxy material (the same material discussed and analyzed in subsections 5.1 and 5.2 of this report), which had *not* been subjected to any heat treatment. It was put through a preparation regimen similar to that described in subsection 4.3 but using available substitutions for expediency: research grade ethanol was used as the organic cleaning solvent, the sandpaper used was 3M brand 236U with P120 grit, and for the "polymer wipe" we used a new Hoya brand eyeglass cleaning cloth made of micropolymer fabric.

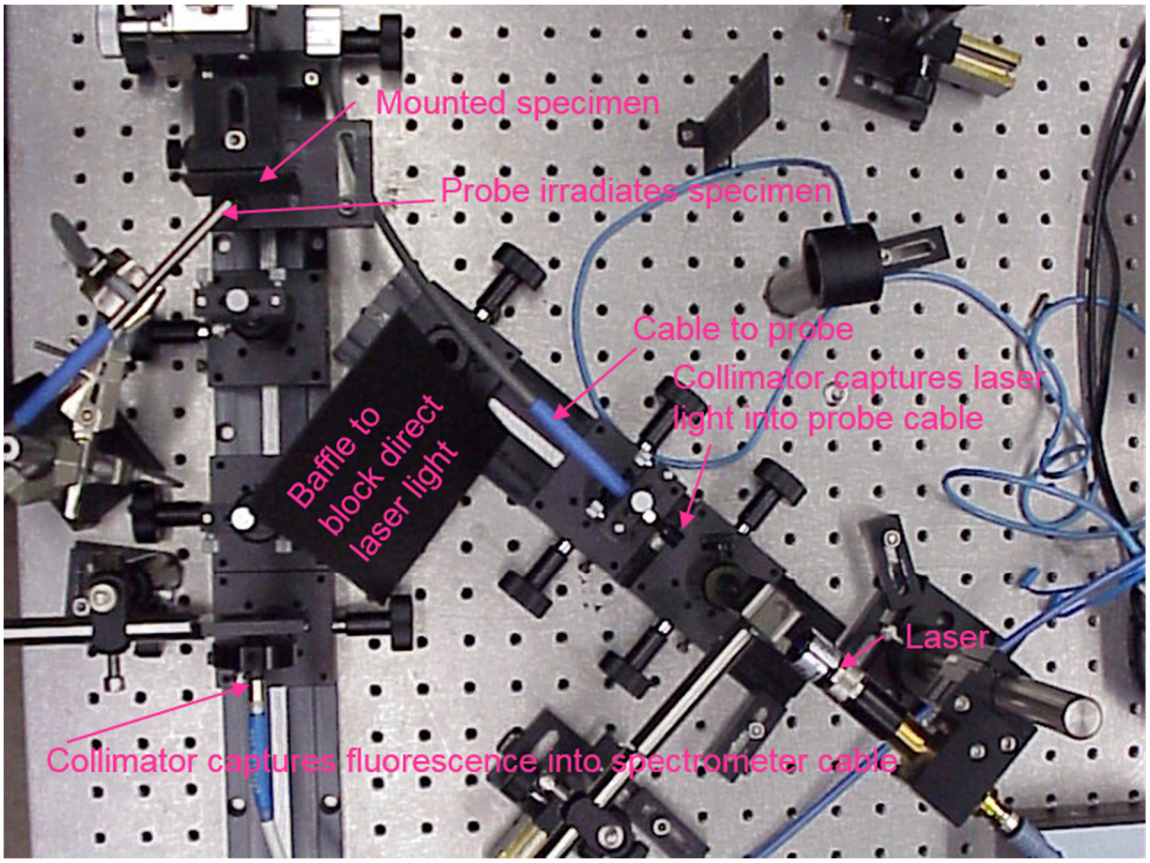

Figure E1. Apparatus Modification for Irradiation Through Optical Fiber. Without repositioning any component of the basic apparatus (Figure 3), we mounted the output cable of an available reflectance probe to intercept the greater part of the laser beam. The probe was mounted to irradiate the specimen through its center-mounted input fiber—thus using the probe's largest-diameter fiber "in reverse". The baffle shown was placed to intercept the portion of the laser beam that would have fallen directly on the specimen.

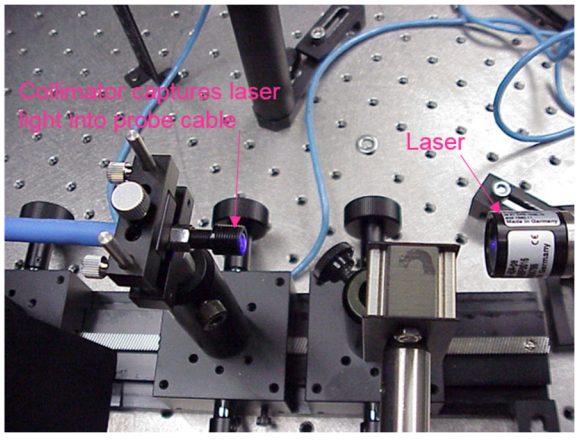

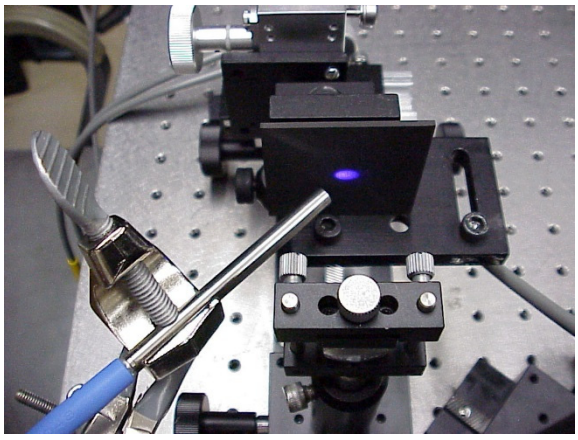

Figure E2. Fiber Cable Intercepting Laser Beam. Figure E3. Specimen Irradiated by Probe.

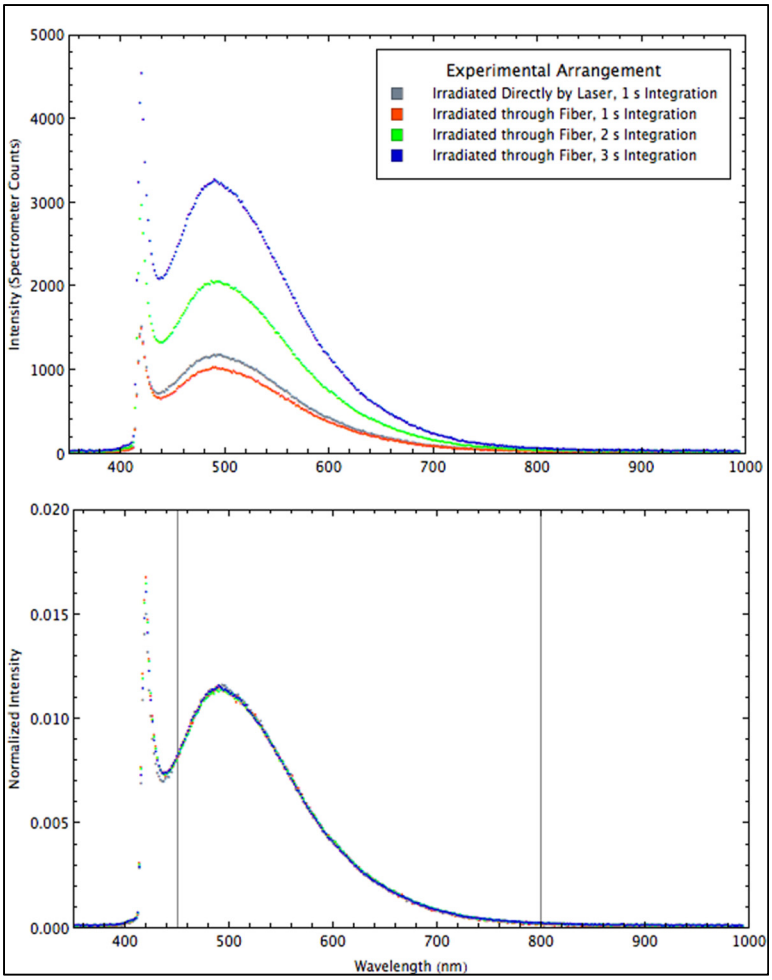

Figure E4. Direct- and Fiber-Irradiated Spectra Compared. The fluorescence intensity under fiber irradiation was slightly lower, as can be seen by comparing the direct irradiation intensity spectrum (gray trace) with the fiber-irradiated spectrum measured using the same one-second integration time. The other two fiber-irradiated spectra were measured with longer integration times and so have higher intensities. Note that the normalized spectra plot virtually on top of each other.